THE JOURNAL OF COMPARATIVE NEUROLOGY 407:207–227 (1999)

Nitric Oxide Synthase in the Guinea Pig Preoptic Area and Hypothalamus: Distribution, Effect of Estrogen, and Colocalization With Progesterone Receptor

MARYVONNE WAREMBOURG,[1]* DANIELE LEROY,[1] AND A. JOLIVET[2]
[1]INSERM U 422, 59045 Lille, France
[2]INSERM U 135, Faculté de Médecine Paris-Sud, Le Kremlin-Bicêtre, France

ABSTRACT

Nitric oxide (NO) may function as an intercellular messenger in the hypothalamus and may play a role in the control of gonadotropin-releasing hormone (GnRH) secretion and sexual behavior. Progesterone also plays an important role in the regulation of reproductive functions. Recent experiments have shown that progesterone-induced sexual behavior in ovariectomized, estrogen-primed rats was caused by the release of NO from nitric oxide synthase (NOS)-containing neurons and the subsequent stimulation of the release of GnRH. To provide further neuroanatomical support for the role of NO in these gonadal steroid-dependent behavioral and physiological processes, we determined (1) the distribution of the nicotinamide-adenosine-dinucleotide phosphate-diaphorase (NADPHd) and NOS enzymes in the guinea pig preoptic area and hypothalamus, regions that contain steroid receptors; (2) the effect of estrogen on NADPHd activity in these regions; and (3) the neuroanatomical relationship between NOS and the progesterone receptor (PR). For this purpose, single- (NADPHd) and double- (NADPHd with NOS or NADPHd with PR or NOS with PR) staining techniques were applied to sections of brains of guinea pigs. The studies showed scattered NADPHd-positive neurons in most parts of the preoptic area and heavily stained cells in the hypothalamus. In these regions, the pattern and density of NOS immunoreactivity closely corresponded to the pattern of NADPHd staining. Quantitative analysis showed an increase in the number of NADPHd-positive neurons in the ventrolateral nucleus of ovariectomized animals primed with estradiol. Approximately 16% of the NOS-immunoreactive (IR) cells in the rostral preoptic area and 55% of NOS-IR cells in the ventrolateral nucleus displayed PR immunoreactivity. These results suggest that NOS may be regulated by gonadal steroids and provide neuroanatomical evidence that progesterone may exert its effect directly on more than half of NOS-synthesizing cells in the ventrolateral nucleus, a key region in the control of sexual behavior. J. Comp. Neurol. 407:207–227, 1999.

Indexing terms: NADPH-diaphorase; histochemistry; immunocytochemistry; diencephalon; NO; steroids

Considerable physiological evidence indicates that the preoptic area and the mediobasal hypothalamus play an important role in neural circuits mediating neuroendocrine-regulated behavioral events associated with reproduction. Progesterone acts in the regulation of these steroid-sensitive functions by binding to specific nuclear receptors in target neurons within the central nervous system. The highest concentrations of estradiol-induced progesterone receptor-immunoreactive (PR-IR) neurons in the guinea pig brain are found in regions that control gonadotropin secretion, in particular the preoptic area and the arcuate nucleus but also in the ventrolateral hypothalamic nucleus (Warembourg et al., 1986; Blaustein et al., 1988; Don Carlos et al., 1989). This latter nucleus has been identified

*Correspondence to: Dr. M. Warembourg, INSERM U 422, 1 Place de Verdun, 59045 Lille Cedex, France. E-mail: warembourg@lille.inserm.fr

Received 14 May 1998; Revised 25 November 1998; Accepted 3 December 1998

as being the principal target site of steroid action for the control of lordosis (Delville and Blaustein, 1991). We previously demonstrated that virtually all estradiol-induced PR-IR neurons in the guinea pig brain also contain estrogen receptors (Warembourg et al., 1989).

To understand how behavior and endocrine events are regulated by progesterone within the preoptic area and the hypothalamus, it is necessary to identify the neurochemicals synthesized by PR-containing cells. Accordingly, we have focused on nitric oxide (NO), a novel type of chemical neuromessenger. NO, which is produced enzymatically in response to an increase in intracellular calcium ions (Garthwaite et al., 1988; Bredt and Snyder, 1990, 1992; Snyder, 1992), has gained increasing interest as an important signal molecule in the brain. This unstable free-radical gas is formed during conversion of the amino acid L-arginine to citrulline by nitric oxide synthase (NOS; Knowles et al., 1989). Neuronal NOS, an isoform constitutively expressed in the nervous system, is dependent on nicotinamide-adenosine-dinucleotide phosphate (NADPH) and is regulated by Ca^{2+}/calmodulin (Bredt and Snyder, 1990; Mayer et al., 1990, 1993; Forstermann et al., 1991). The distribution of NOS correlates with the described distribution of NADPH-diaphorase (NADPHd) activity (Dawson et al., 1991; Hope et al., 1991), which makes it possible to localize NOS with a specific histochemical method by using β-NADPH as the substrate. This diaphorase activity is able to transfer electrons from NADPH to tetrazolium salts used as a chromogen that produces an insoluble dark-blue formazan precipitate (Thomas and Pearse, 1961; Kuonen et al., 1988).

Mapping studies, more or less detailed, on the distribution of NADPHd and/or NOS have reported that distinct subgroups of neurons and fiber systems stain for NADPHd and/or NOS within the brain of mammals such as cats (Mizukawa et al., 1989), rats (Vincent and Kimura, 1992; Rodrigo et al., 1994), and humans (Egberongbe et al., 1994). However, to our knowledge, there are no published studies that have examined the distribution of NOS-positive neurons in the guinea pig hypothalamus. Although NADPHd activity and NOS immunoreactivity show the same population of neurons (Dawson et al., 1991; Hope et al., 1991), some doubts still exist concerning the complete overlap of NADPHd-positive neurons and NOS-immunoreactive (NOS-IR) neurons in certain structures of brain (Schmidt et al., 1992; Valtschanoff et al., 1993; Kharazia et al., 1994).

NO functions as an intercellular messenger molecule in hypothalamic systems involved in the regulation of neuroendocrine events. Based on in vitro and in vivo studies using NO activators or inhibitors, NO influences the release of gonadotropin-releasing hormone (GnRH; Moretto et al., 1993; Rettori et al., 1993). However, GnRH-containing neurons themselves have not been found to express NOS but are frequently surrounded by NOS-containing neurons (Herbison et al., 1996), whereas colocalization of NADPHd staining and estrogen receptor has been reported in a subpopulation of neurons in the rat preoptic area (Okamura et al., 1994a). Moreover, in the ventrolateral subdivision of the ventromedial nucleus of the rat, estrogen treatment increases neuronal NOS mRNA (Ceccatelli et al., 1996) and prominent NADPHd staining has been described in males (Vincent and Kimura, 1992) and in females (Okamura et al., 1994b). This region is analogous to the ventrolateral hypothalamic nucleus of the guinea pig. In addition, other studies have demonstrated the involvement of NO in the regulation of sexual behavior in male mice (Nelson et al., 1995) and in the mediation of progesterone-facilitated lordosis in female rats (Mani et al., 1994). The aim of these studies was to determined whether NOS is colocalized with estradiol-induced PR immunoreactivity and, therefore, by implication with estrogen receptor immunoreactivity.

In the present study, we described the localization of NADPHd-positive neurons in the guinea pig preoptic area and hypothalamus and mapped their distribution in detail. To make certain that the NADPHd staining shows neuronal structures that contain NOS, we performed NADPHd histochemistry in combination with immunocytochemistry by using an antibody against neuronal NOS on the same sections. We then investigated the effects of estrogen on NADPHd activity in a few regions, especially those known to contain progesterone binding sites. Lastly, we provided anatomical evidence for an association of NOS and PR by combining PR immunocytochemistry with either NOS immunocytochemistry or NADPHd histochemistry.

MATERIALS AND METHODS

Animals and treatments

The present study is based on 44 adult female Hartley guinea pigs weighing 400–450 g, obtained from CEGAV (St Mars d'Egrenne, France). The guinea pigs were group housed on a 14:10 light: dark cycle, with food and water available ad libitum. All animal experiments were carried out in accordance with the European Communities Council Directive of 24 November 1986 (86/609/EEC).

Abbreviations

AA	anterior hypothalamic area
ac	anterior commissure
Ar	arcuate nucleus
BM	basal nucleus of Meynert
cp	cerebral peduncle
DBh	horizontal portion of nucleus of diagonal band of Broca
DBv	vertical portion of nucleus of diagonal band of Broca
Dm	dorsomedial nucleus
f	fornix
LA	lateral hypothalamic area
LPA	lateral preoptic area
Ma	medial mamillary nucleus, anterior division
MP	medial preoptic nucleus
MPA	medial preoptic area
mt	mamillothalamic tract
oc	optic chiasm
ot	optic tract
PA	posterior hypothalamic area
Pea	periventricular nucleus, anterior portion
Pep	periventricular nucleus, preventricular portion
Pm	paramamillary nucleus
PV	paraventricular nucleus
Sc	suprachiasmatic nucleus
SI	substantia innominata
So	supraoptic nucleus
ST	nucleus of stria terminalis
T	tuberal nucleus
V	ventricle
Vl	ventrolateral nucleus
Vm	ventromedial nucleus
VP	ventral premamillary nucleus

All animals were ovariectomized (OVX) through bilateral dorsal incisions under a combination of ketamine (8 mg/kg) and xylazine (40 mg/kg) anesthetics that were given intramuscularly and were allowed to recover for at least 10 days prior to subsequent hormone treatment. Thirty-six guinea pigs were used for NADPHd histochemistry in the study of the effects of estrogen on NADPHd activity. OVX animals were injected subcutaneously either with 15 µg of estradiol benzoate (EB) dissolved in 0.25 ml of sesame oil daily for 1 (n = 4), 2 (n = 4), 3 (n = 4), 5 (n = 4), or 7 (n = 4) days or with an oil vehicle daily for 3 (n = 4), 5 (n = 4), or 7 (n = 4) days prior to perfusion. Two guinea pigs were used for NOS immunocytochemistry combined with NADPHd histochemistry, and on the other animals a combined NADPHd/PR or NOS/PR immunocytochemical procedure was applied. For these latter experiments, the OVX animals received EB subcutaneously daily for 5 days prior to perfusion.

Tissue preparation

Animals were deeply anesthetized with ketamine plus xylazine and transcardially perfused by using an intraventricular catheter attached to a peristaltic pump. Animals were perfused with 100 ml of heparinized 0.9% saline followed by 500 ml of cold 4% paraformaldehyde in a 0.1 M sodium phosphate buffer (PB), pH 7.4. Each brain was dissected and the diencephalic regions were postfixed in the same solution for 3 hours at 4°C and then soaked in 15% buffered sucrose (pH 7.4) at 4°C for at least overnight. The tissues were either cut immediately on a freezing microtome into cross sections at a thickness of 60 µm, which reacted in free-floating state, or were frozen by immersion in liquid nitrogen-cooled isopentane and stored at −80°C until sectioning. The frozen tissues were then cut into cross sections at a thickness of 20 µm in a cryostat at −20°C. Sections were thaw mounted on gelatin-coated slides and processed for immunostaining or stored at −80°C until further processing. Cross sections ranging from the organum vasculosum of the lamina terminalis to the premamillary region, corresponding to sections 229–375 of the guinea pig atlas of Bleier (1983), were processed for NADPHd staining or immunostaining as follows.

NADPHd histochemistry

The NADPHd histochemistry was carried out as previously described (Vincent and Kimura, 1992) on free-floating sections for the mapping of positive neurons and for the study of the effect of estrogen on NADPHd activity. Sections were washed three times for 10 minutes in 0.1 M PB, pH 7.4. They were then incubated in 0.1 M PB (pH 7.4) containing 1.1 mM β-NADPH (Boehringer-Mannheim, Meylan, France), 0.1 mM nitroblue tetrazolium (NTB; Sigma, Saint Quentin Fallavier, France), and 0.3% Triton X-100 at 37°C for 1 hour. After incubation, the sections were rinsed in 0.01 M sodium phosphate buffered saline (PBS) at pH 7.4, put on gelatin-coated glass slides, air dried overnight, and coverslipped with glycergel (Dako, S.A., Trappes, France).

Primary antisera

A polyclonal antibody to rat brain NOS (kindly provided by Prof. J.M. Polak, London, U.K.) was used at a dilution of 1:1,000. NOS was purified from whole rat brain according to the method of Bredt and Snyder (1990) and injected into rabbits as described elsewhere (Springall et al., 1992; Riveros-Moreno et al., 1993). This antiserum has been shown to react immunocytochemically with neurons from different species (Springall et al., 1992; Terenghi et al., 1993; Martinez et al., 1994).

The antibody used to detect the PR was let 126, a monoclonal antibody raised in a mouse against rabbit uterine receptors. A working dilution of 1.5 µg/ml was used. The characteristics and specificity of this antiserum have been previously described (Logeat et al., 1983, 1985; Loosfelt et al., 1984; Lorenzo et al., 1988).

Double labeling for NOS and NADPHd

In two animals, some series of cryostat sections throughout the preoptic area and hypothalamus were processed for NOS immunocytochemistry. The sections first were rinsed three times for 10 minutes in PBS and then incubated for 70 hours at 4°C in a humid atmosphere, with the polyclonal anti-NOS antibody diluted in PBS containing 0.3% Triton X-100 and 10% normal donkey serum to diminish nonspecific staining. NOS immunoreactivity was demonstrated by incubating the sections in fluorescein-conjugated donkey anti-rabbit immunoglobulins (Amersham, Les Ulis, France) diluted 1:50 for 1 hour 30 minutes at 4°C. The sections were then coverslipped with glycerol PBS (3:1, v/v) and photographed. At this point, the coverslips of photographed sections were carefully removed and the sections were processed for NADPHd staining as described above.

Double labeling for PR and NADPHd

In two animals, free-floating sections were incubated for 70 hours at 4°C in the monoclonal anti-PR antibody diluted in PBS containing 10% normal sheep serum. PR immunoreactivity was demonstrated by incubating the sections in biotinylated sheep anti-mouse immunoglobulins (dilution 1:200; Amersham) for 1 hour at room temperature and then in streptavidin peroxidase (dilution 1:100; Amersham) for 1 hour at room temperature. The final staining was made with 0.5 mg/ml 3,3′-diaminobenzidine tetrahydrochloride (Research Organics Inc., Cleveland, OH) in the presence of 0.03% hydrogen peroxide for 30–45 minutes. Subsequently, the histochemical technique for NADPHd was performed on the same sections, as described above. The sections were then rinsed in PBS, mounted on glass slides, air dried, dehydrated, and coverslipped with Eukitt (O. Kindler GmbH and Co., Freiburg, Germany).

Double labeling for NOS and PR

In four guinea pigs, cryostat sections were incubated for 30 minutes at room temperature in PBS containing 10% normal sheep serum and 10% normal donkey serum. After rinsing three times in PBS, the sections were incubated for 70 hours at 4°C in a humid atmosphere in a cocktail of the primary antibodies (anti-PR and anti-NOS) described previously. The sections were then processed as above for NOS immunostaining. PR immunoreactivity was demonstrated by incubating the sections in biotinylated sheep anti-mouse immunoglobulins (dilution 1:200; Amersham) for 1 hour 30 minutes at 4°C, and then in Texas red–streptavidin (dilution 1:200; Amersham) for 1 hour at 4°C. The sections were coverslipped with glycerin:PBS (3:1, v/v) containing 0.1% *p*-phenylenediamine to avoid fading.

Specificity of the stainings

On control sections subjected to the NADPHd reaction, no NADPHd staining was observed when β-NADPH substrate or NTB was omitted from the incubation medium. No immunolabeling was observed when sections were incubated with NOS antiserum preabsorbed (overnight at 4°C) with the antigen extracted from rat brain. Sections were also incubated with monoclonal anti-PR antibody that had been preabsorbed before the immunostaining procedure with highly purified PR (Warembourg et al., 1986). Neither nuclear staining for PR nor NOS immunoreactivity was obtained when (1) primary antibodies were omitted, (2) primary antibodies were replaced by normal mouse or rabbit serum, and (3) a second antiserum was used after the primary antibody raised in an inappropriate species.

Presentation and analysis of results

Observation, evaluation, and photomicrography of sections were done by using a Leica microscope (Model DMRB) fitted with filters for both brightfield and fluorescence microscopy. Two adjacent sets of cross sections were used to chart in detail the distribution of NADPHd-positive neurons in the preoptic area and hypothalamus (Figs. 1, 2). One set was stained with thionin only and the other was stained with NADPHd histochemistry. The comparison of NADPHd-stained sections with those stained by thionin showed that NADPHd neurons were not confined to cytoarchitectonic regions as defined by Nissl staining. Therefore, the boundaries of classically defined brain nuclei were not marked on these maps, but their general location has been indicated according to the terminology used by Bleier (1983).

To evaluate whether there was a difference in the NADPHd activity as a function of the period of the steroid treatment compared with the level seen in OVX females, the number of NADPHd-positive neurons was determined in the different treatment conditions with the steroid or with the oil vehicle. Counting was done manually under a microscope, with a 40× objective, by an experimenter unaware of the endocrine condition of the subjects. Cells were counted throughout the rostrocaudal extent of four brain areas: the preoptic area, the paraventricular nucleus, the ventrolateral nucleus, and the posterior region of the arcuate nucleus (Fig. 8). Care was taken to ensure that the same cell populations for a given region were analyzed for all brains. Regions counted were standardized by reference to the atlas (Bleier, 1983) as follows: every second hemisection was analyzed between sections 242 and 267 of the atlas for the preoptic area, between sections 291 and 308 for the paraventricular nucleus, between sections 322 and 357 for the ventrolateral nucleus, and between sections 357 and 370 for the posterior region of the arcuate nucleus. In the preoptic area, three main populations of NADPHd-positive neurons were considered: (1) clusters of neurons located periventricularly in the preventricular portion of the periventricular nucleus, (2) clusters of neurons located ventrally above the optic chiasm in the medial preoptic nucleus, and (3) groups of neurons located laterally in the medial preoptic area. In the paraventricular nucleus, all positive neurons were considered independently of their size and of the subdivision (magnocellular or parvicellular) in which they were located. Measurements of NADPHd-positive cells in the ventrolateral nucleus were taken from the most rostral to the most caudal parts of this nucleus. Measurements within the arcuate nucleus were concentrated in its posterior aspect, where NADPHd-positive cells were most abundant. Four animals were analyzed in each experimental condition: OVX, OVX + five periods of treatment with EB (24 and 48 hours and 3, 5, and 7 days), and OVX + three periods of treatment with the oil vehicle (3, 5, and 7 days) for each region. A cell was considered NADPHd-positive if a purplish blue reaction product was present within its cytoplasm. Cell counting per animal was carried out on hemisections: nine in the preoptic area, four in the paraventricular nucleus, 10 in the ventrolateral nucleus, and five in the arcuate nucleus. The values given were means ± S.E.M. Statistical analysis was carried out with the SigmaStat 1.0 software (Jandel Scientific GmbH, Erkrath, Germany) for the four brain regions. The significance of the EB treatment was assessed with an one-way analysis of variance by using the Kolmogorov-Smirnov test ($P < 0.01$) for normality and the Levene Median test ($P < 0.01$) for equal variance. For appropriate post hoc analyses, the Bonferroni t-test was performed with a significance level of 95% ($P < 0.05$).

Fluorescence sections were viewed under the microscope equipped with appropriate Pleomopak filters. Fluorescein-labeled neurons were observed under an L4 filter (450–490 nm) and Texas red-labeled neurons were examined with an N2.1 filter (515–560 nm). Identification of double-labeled cells was made by switching from one filter cube to the other during the observation or with a BGR filter (400/20, 495/15, and 570/50 nm) that allowed simultaneous visualization of fluorescein and Texas red. To provide an estimate of the double-IR cell population (Table 1), we counted all PR-IR, NOS-IR, and PR-IR + NOS-IR neurons within the boundaries of the preoptic area and ventrolateral nucleus determined on the basis of the PR immunostaining. Sections were analyzed through the rostrocaudal extent of the entire regions, which were divided into three anatomical levels with reference to the atlas. For the preoptic area, the rostral level was placed between sections 242 and 253, the medial level between sections 253 and 262, and the caudal level between sections 262 and 271. For the ventrolateral nucleus, the rostral level was situated between sections 322 and 337, the medial level between sections 337 and 349, and the caudal level beyond section 349. Only cells in which the nucleus was visible were considered. Cell counting was carried out in four animals on 12 hemisections for each level. Every second hemisection was analyzed, and cells were manually counted under a microscope at a 40× objective magnification. Quantitative data were expressed as means (±S.E.M.) of cell profiles per animal. From these raw data, we then calculated the percentage of the NOS-IR cells that contained PR and the percentage of the PR-IR cells that contained NOS.

RESULTS

Distribution of NADPHd-positive neurons

The extent of NADPHd activity in the diencephalic regions was assessed on free-floating sections of the brain from OVX and estrogen-treated guinea pigs. Neuronal cell bodies and fibers exhibiting NADPHd staining were found in particular nuclei throughout the preoptic area and hypothalamus. The soma, dendrites, and axons were

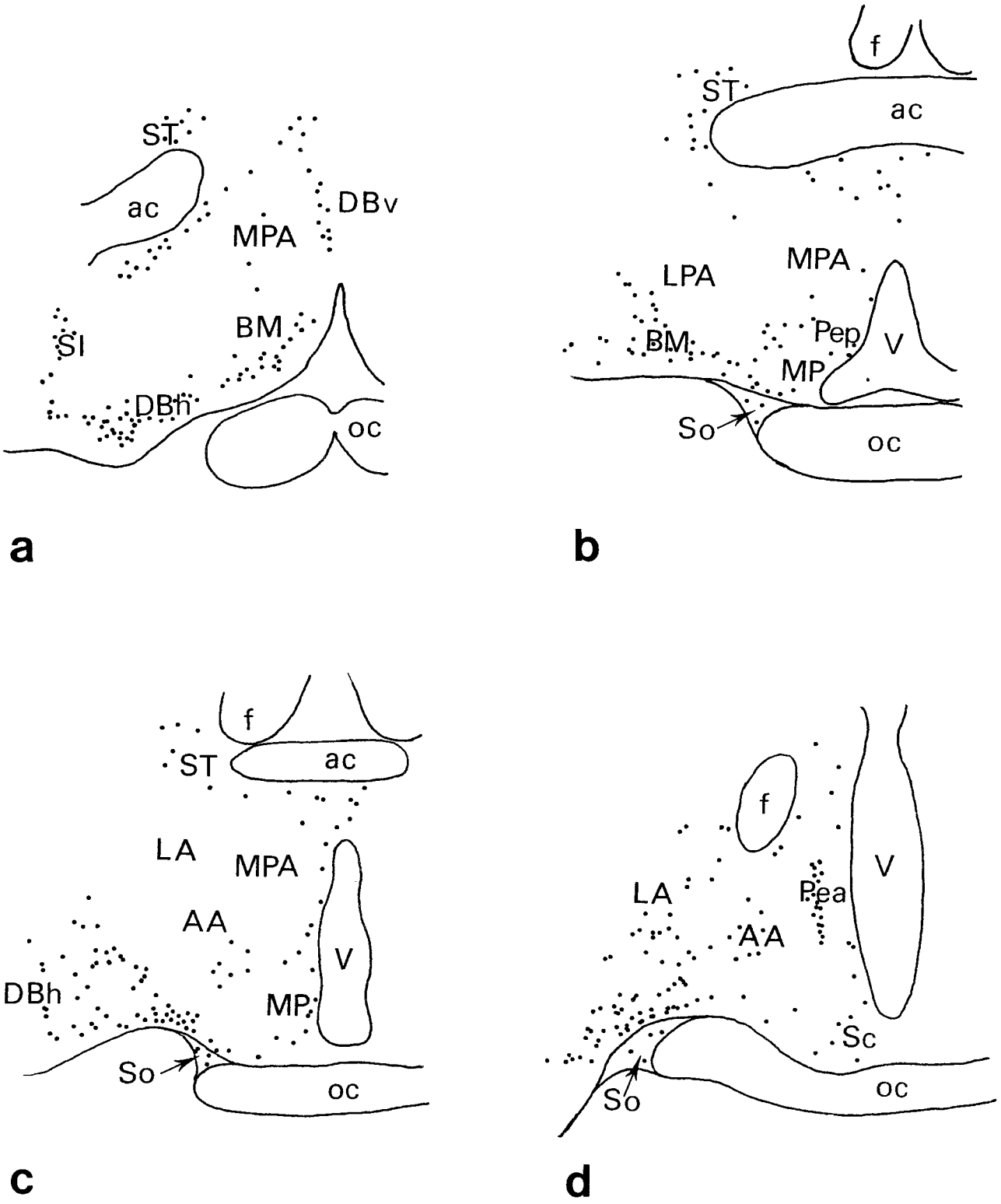

Fig. 1. **a–d:** Schematic drawings of cross sections from rostral (a) to caudal (d) through the preoptic area of the guinea pig showing the distribution of nicotinamide-adenosine-dinucleotide phosphate diaphorase (NADPHd)-positive cells. Each dot represents one NADPHd-positive cell. For abbreviations, see list.

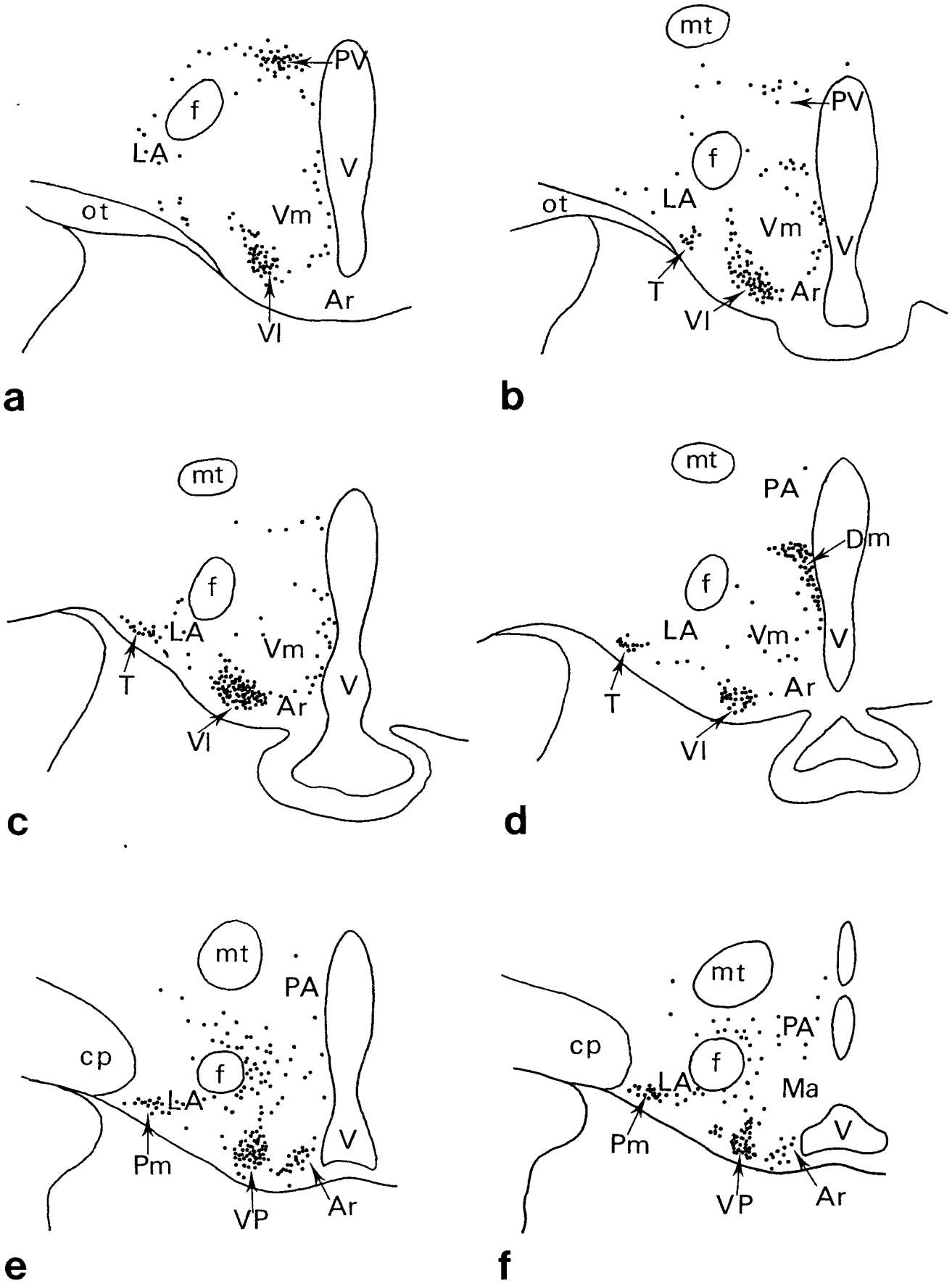
PV
f
LA
V
ot
Vm
Ar
Vl
a
mt
PV
f
ot
LA
Vm
V
T
Ar
Vl
b
mt
f
LA
Vm
T
V
Ar
Vl
c
mt
PA
Dm
f
LA
Vm
V
T
Ar
Vl
d
mt
PA
cp
f
LA
V
Pm
VP
Ar
e
mt
cp
PA
f
LA
Ma
V
Pm
VP
Ar
f

Figure 2

TABLE 1. Estimation of the Number of Progesterone Receptor-Immunoreactive (PR-IR), Nitric Oxide Synthase-Immunoreactive (NOS-IR), and Double-Immunoreactive (PR-IR + NOS-IR) Neurons in Different Regions of the Preoptic Area and Ventrolateral Nucleus[1]

Regions	Number of PR-IR neurons	Number of NOS-IR neurons	Number of PR-IR + NOS-IR neurons	%NOS-IR neurons with PR	%PR-IR neurons with NOS
Preoptic area					
Rostral level	2,809 ± 46	152 ± 7	25 ± 2	16.70 ± 0.80	0.90 ± 0.08
Medial level	3,080 ± 88	199 ± 11	13 ± 1	6.81 ± 0.77	0.44 ± 0.05
Caudal level	1,861 ± 99	231 ± 5	15 ± 2	6.45 ± 0.91	0.80 ± 0.11
Ventrolateral nucleus					
Rostral level	870 ± 44	338 ± 21	186 ± 10	55.10 ± 1.17	21.40 ± 0.17
Medial level	1,010 ± 38	349 ± 12	186 ± 7	53.40 ± 1.37	18.50 ± 0.41
Caudal level	886 ± 67	365 ± 23	210 ± 17	57.30 ± 1.15	23.80 ± 1.16

[1]The values represent mean number (±S.E.M.) of cells counted in 12 hemisections from each region (n = 4).

stained, but not the nucleus. There was considerable heterogeneity in the morphology of the NADPHd-reactive neurons. There were also differences noted in the intensity of staining between neurons, which differed from pale to very dark. Many neurons such as those in the cortex and in the striatum were stained in a Golgi-like manner, with the cell body and dendrites filled with dense reaction product. Other neurons including neurons in the mediobasal hypothalamus were moderately stained, whereas other neurons, such as preoptic cells, showed a rather lower staining intensity of the perikarya and dendrites. However, there was no difficulty in distinguishing between the stained and unstained neurons. No reaction was observed in control sections when β-NADPH or NTB was omitted from the incubation solution.

A rostral-to-caudal series of cross sections from one representative brain reacted for NADPHd histochemistry was used to chart in detail the preoptic area and hypothalamus (Figs. 1, 2). Dots illustrate the distribution of NADPHd-positive neurons, but fibers are not depicted. The following description is also limited to NADPHd staining in neurons. Although the results are described from OVX animals treated with EB for 5 days, a basically similar distribution of staining within the preoptic area and hypothalamus was observed in all hormonal conditions.

Preoptic area

In the most rostral regions of the preoptic area (Fig. 1a), a considerable number of well-stained NADPHd cells were in the nucleus of the diagonal band of Broca, primarily in its horizontal portion. These neurons were observed in groups of two or three layers. They extended caudally toward the basal nucleus of Meynert and the substantia innominata. The region of the lamina terminalis contained many weakly stained neurons. Clusters of NADPHd neurons were seen rostral to and below the anterior commissure (Fig. 1a–c). Many cells in the nucleus of the stria terminalis were weakly stained (Fig. 1a–c). Only a few small neuronal somata that showed weak staining for NADPHd were found scattered in the medial preoptic and preoptic periventricular nuclei, some just beneath the ependymal layer (Figs. 1b,c, 3a). Weakly stained neurons were widely dispersed in the medial preoptic area and its surrounding region (Figs. 1a-c, 3b), with the exception of a caudal cluster that ran parallel to the third ventricle (Fig. 1d). The weakness of the staining within these preoptic regions did not appear to be due to a methodological problem because cells in the surrounding areas stained strongly. In the dorsal portion of the preoptic area, loosely scattered NADPHd-positive neurons were constantly seen close to the top of the ventricle and between the ventricle and the anterior commissure (Fig. 1b,c). Within the supraoptic nucleus, about a third of the neurons were weakly stained, whereas the others were unstained (Fig. 1b-d). Many well-stained neurons were detected above the supraoptic nucleus (Fig. 3c) and ran dorsally into the lateral preoptic area and more caudally into the lateral and anterior hypothalamic areas (Fig. 1b–d). Some moderately stained cell bodies were seen around the suprachiasmatic nucleus (Fig. 1d).

Hypothalamus

In the lateral hypothalamic area, there were large numbers of intensely positive small neurons (Fig. 2a–f). These cells extended dorsally and merged with the perifornical area. The magnocellular elements of the paraventricular nucleus showed a dense accumulation of reaction product (Figs. 2a,b, 4a). In the periventricular hypothalamic region, several small cells, frequently parallel to the third ventricle, were weakly stained. Groups of small cells, weakly to moderately stained, were found in the dorsomedial nucleus just dorsal to the ventromedial nucleus between the fornix and the ventricle (Figs. 2d, 4b). Few NADPHd-positive neurons were seen within the ventromedial nucleus, but small stained neurons were found outside of the well-defined boundaries of the nucleus (Figs. 2a–c, 5a). The ventrolateral nucleus contained a conspicuous population of NADPHd-positive neurons (Figs. 2a–d, 5b). The positive cells were densely packed throughout the rostrocaudal extent of the nucleus and embedded in a network of strongly stained fibers and puncta (Fig. 6a). These cells were darkly stained but less Golgi-like than those in the extrahypothalamic regions such as the cortex. NADPHd-positive neurons were occasionally observed in the anterior (Fig. 6b) and median portions of the arcuate nucleus, whereas, at more caudal level, moderately stained cell bodies occurred in the region close to the lateral wall of the third ventricle (Figs. 2e,f, 6c). The ventral premamillary nucleus was demarcated by an intense diffuse reaction product that included neurons intermingled with fibers and dendritic processes (Figs. 2e,f, 7a). Clusters of well-stained cells were also present throughout the area of the tuber cinereum including the medial and lateral divisions of the tuberal nucleus (Figs. 2b–d, 7b). Caudally, these groups are continuous with NADPHd-positive cells in the ventral part of the paramamillary nucleus (Fig.

Fig. 2. **a–f:** Schematic drawings of cross sections from rostral (a) to caudal (f) through the hypothalamus of the guinea pig showing the distribution of nicotinamide-adenosine-dinucleotide phosphate diaphorase (NADPHd)-positive cells. Each dot represents one NADPHd-positive cell. For abbreviations, see list.

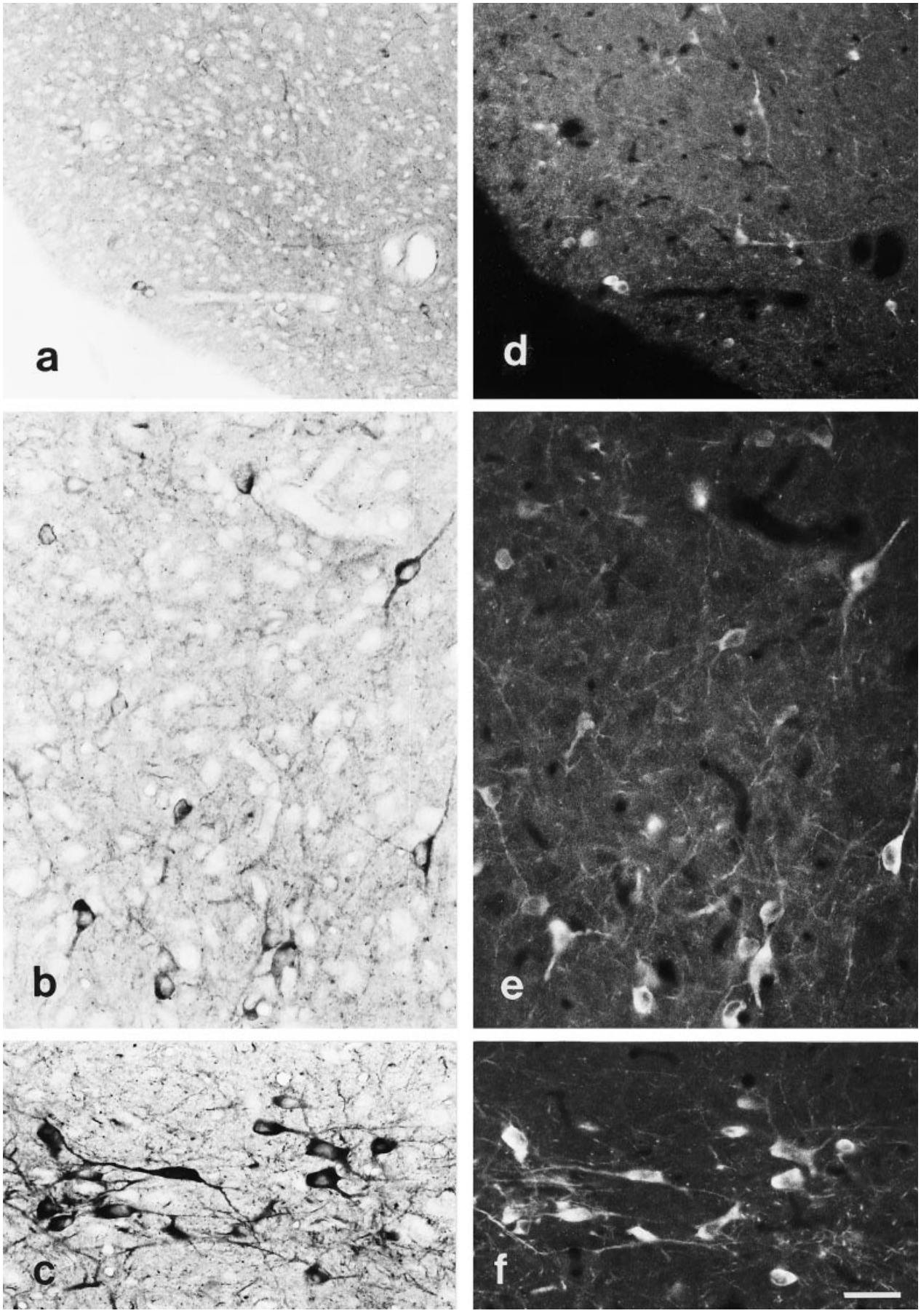

Figure 3

2d–f). The posterior hypothalamic area contained a limited number of NADPHd-positive neurons (Fig. 2e,f).

Correlation between NOS-IR and NADPHd-positive neurons

The distribution of NOS within the preoptic area and hypothalamus was determined by immunolabeling with an antiserum against neuronal NOS. Both perikarya and processes were immunostained. As shown in Figures 3–7, the location, number, and morphology of NOS-IR neurons were similar to those of neurons stained for NADPHd as described above. In the preoptic area, NOS-IR neurons in the medial preoptic nucleus (Fig. 3d) and in the medial preoptic area (Fig. 3e) displayed weak to medium fluorescence in comparison with those observed in the neighboring structures including the caudate nucleus, the horizontal limb of the nucleus of the diagonal band of Broca, and the region just dorsal to supraoptic nucleus (Fig. 3f). In the hypothalamus, NOS-IR cells were distributed heterogeneously. The magnocellular neurons of the paraventricular nucleus (Fig. 4c) were strongly immunoreactive, and many positive cells were found in the dorsomedial nucleus (Fig. 4d) and around the ventromedial nucleus (Fig. 5c). The ventrolateral nucleus harbored the most immunoreactivity for NOS in the guinea pig hypothalamus (Figs. 5d, 6d). The anterior and median portions of the arcuate nucleus (Fig. 6e) were practically negative, in striking contrast to the posterior region that contained a group of NOS-IR cells (Fig. 6f). Intensely immunoreactive neurons were also present in the ventral premamillary nucleus (Fig. 7c) and in the tuberal nucleus (Fig. 7d). When the distribution of NOS-IR neurons was compared on photomicrographs with that of NADPHd-reactive neurons in the same brain section, the profiles of the cell bodies matched exactly with the two staining methods (Figs. 3–7). Not only was a one-to-one correlation between the locations of the NOS- and NADPHd-positive neurons observed, but even the relative staining intensities were found to be similar.

Effect of estrogen on NADPHd activity

In both OVX guinea pigs and OVX guinea pigs primed with EB, many heavily stained NADPHd-positive neurons were found in the ventrolateral nucleus and the paraventricular nucleus, whereas a limited number of moderately stained neurons was observed in the preoptic area and the posterior part of the arcuate nucleus. In the preoptic area (Fig. 8a) and the paraventricular nucleus (Fig. 8b), no change in neuronal staining intensity or any significant change in the cell counts could be observed between the OVX guinea pigs and OVX guinea pigs treated with EB, whenever the time of estrogen treatment. Conversely, an increase in the number of NADPHd-positive neurons was seen in the ventrolateral nucleus in all OVX animals primed with EB for 1–7 days (Fig. 8c). Although quantitative analysis showed an increase through the extent of the ventrolateral nucleus, cell counts of NADPHd-reactive neurons showed no significant difference when OVX guinea pigs treated with EB for 1–3 days were compared with OVX guinea pigs. Five days after EB treatment, the number of NADPHd-positive neurons in the ventrolateral nucleus was significantly increased ($P < 0.05$) to 1.5-fold that of OVX 5 and 7 days after treatment. Some variation in staining intensity among neurons was also observed. Most neurons were generally strongly stained. The number of NADPHd-positive cells 7 days after EB did not differ remarkably from that of animals treated for 5 days. The number of stained neurons in the ventrolateral nucleus of EB-primed females was also significantly higher than that of OVX females treated with an oil vehicle, but the statistical analysis of cell counts did not show a significant difference between OVX animals and OVX animals treated with the vehicle (Fig. 8c). In the posterior region of the arcuate nucleus, the neuronal staining was not altered significantly by treatment with EB (Fig. 8d). Although cell counts of EB-treated animals were somewhat higher than those of OVX animals, quantitative analysis showed no significant difference irrespective of the time of the EB treatment.

Colocalization of NADPHd/NOS and PR

The distribution of PR-IR neurons observed in the present study corresponded well with that reported in previous studies (Warembourg et al., 1986, 1989). Briefly, PR-IR perikarya were abundant in the entire medial preoptic nucleus (Fig. 9a,b) and the preoptic periventricular nucleus extending in columns parallel to the ventricular surface (Fig. 9c). Within the hypothalamus, PR-IR cells were observed throughout the rostrocaudal extent of the arcuate (Fig. 10a) and ventrolateral nuclei (Fig. 10b,c). Two different procedures, NADPHd histochemistry combined with PR immunocytochemistry or double immunofluorescence (PR + NOS) immunocytochemistry, were used to detect the presence of PR and NOS in the same sections. With the first procedure, NADPHd-positive neurons contained a dark-blue-stained cytoplasm and the PR-IR neurons had a brown cell nucleus (Fig. 11a,e). With the second procedure, PR immunoreactivity was restricted to the nucleus, which displayed a red fluorescence from Texas red, whereas NOS immunoreactivity was seen in the cytoplasm as a yellow-green fluorescence (Fig. 11b–d). Double immunofluorescence, applied on cryostat sections, was used for quantitative analysis, whereas NADPHd histochemistry and PR immunocytochemistry, employed on free-floating sections, allowed us to have an unequivocal confirmation of the localization of the two markers. In the latter procedure, although immunolabeling appeared throughout the entire thickness of the sections, it is possible that some deep PR-IR neurons could not be detected, so the number of double-labeled cells could be underestimated. The present results were obtained from OVX animals primed with EB for 5 days to induce PR immunoreactivity. A comparison of PR-stained material with NOS-stained material showed close relationships between labeled neuronal structures in certain regions of the preoptic area and hypothalamus. Figures 9 and 10 depict the degree of overlap of PR staining and NOS staining. PR-IR neurons located in the preoptic area were densely packed and appeared to be more homogeneously distributed than NOS-IR cells (Fig. 9a–f). A closer examination of this area showed that at the rostral level NOS-IR cells (Fig. 9d,e) were loosely arranged and were inter-

Fig. 3. Localization of nitric oxide synthase with nicotinamide-adenosine-dinucleotide phosphate diaphorase histochemistry (**a–c**) and immunocytochemistry (**d–f**). Pairs of photomicrographs illustrate the same sections where the correlation between the two stainings is demonstrated in the medial preoptic nucleus (a,d), the medial preoptic area (b,e), and the region just dorsal to the supraoptic nucleus (c,f). Scale bar = 125 μm for a,d, 32 μm for b,c,e,f.

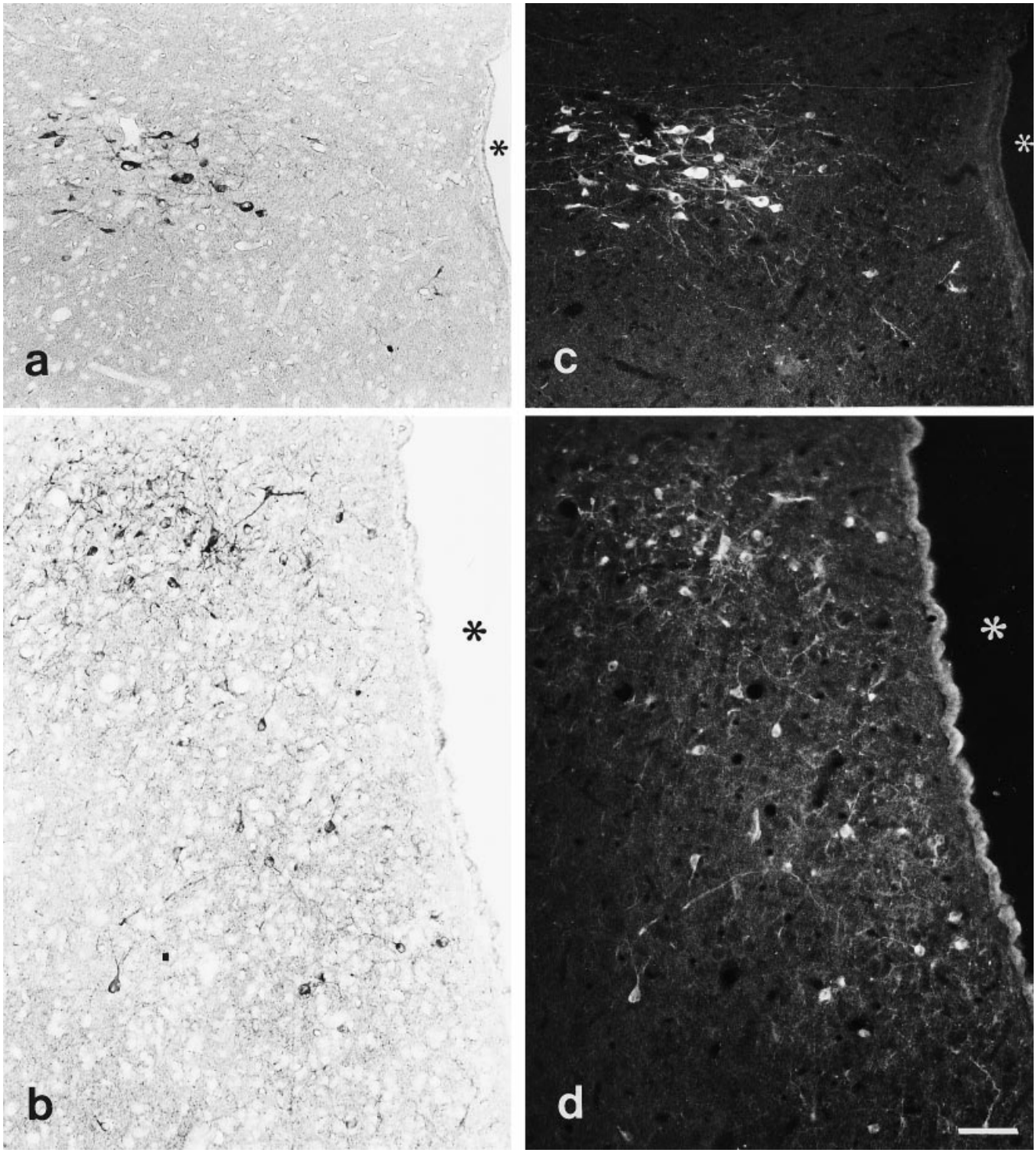

Fig. 4. Localization of nitric oxide synthase with nicotinamide-adenosine-dinucleotide phosphate diaphorase histochemistry (**a,b**) and immunocytochemistry (**c,d**). Pairs of photomicrographs show identical sections where the correlation between the two stainings is seen in the paraventricular nucleus (a,c) and the dorsomedial nucleus (b,d). Asterisk, third ventricle. Scale bar = 85 µm for a,c, 63 µm for b,d.

mingled with PR-IR cells in the medial preoptic nucleus, whereas at a more caudal level PR-containing cells in the preoptic periventricular nucleus were rather separated from those immunoreactive for NOS (Fig. 9f). Therefore, double-IR cells were most abundant at the anterior level. Our quantitative analysis showed that approximately 16%

Fig. 5. Localization of nitric oxide synthase with nicotinamide-adenosine-dinucleotide phosphate diaphorase histochemistry (**a,b**) and immunocytochemistry (**c,d**). Photomicrographs of pairs of sections show reactive cells outside of the well-defined boundaries of the ventromedial nucleus (a,c) and throughout the ventrolateral nucleus (b,d). Vm, ventromedial nucleus; asterisk, third ventricle. Scale bar = 62 µm.

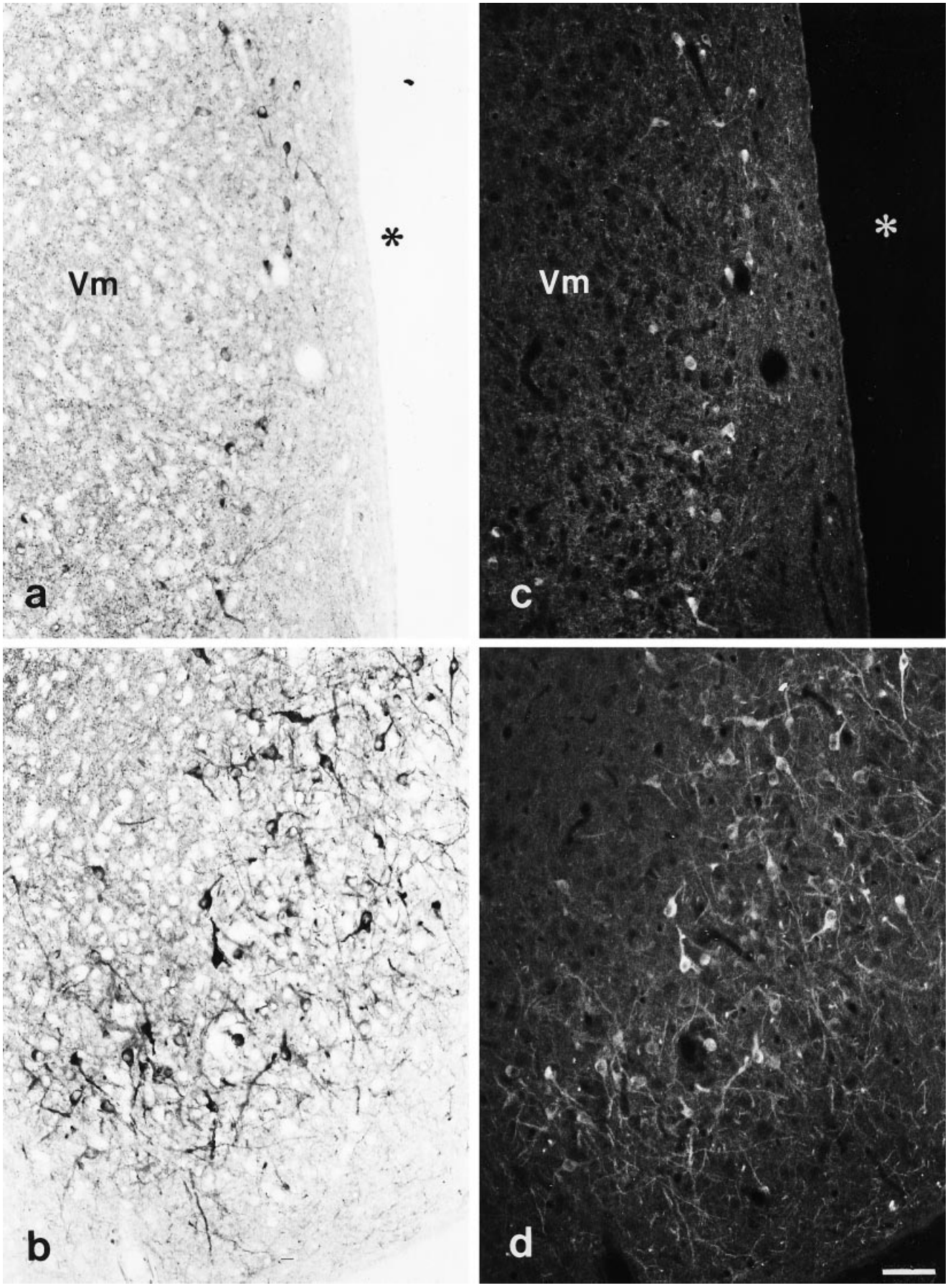

Figure 5

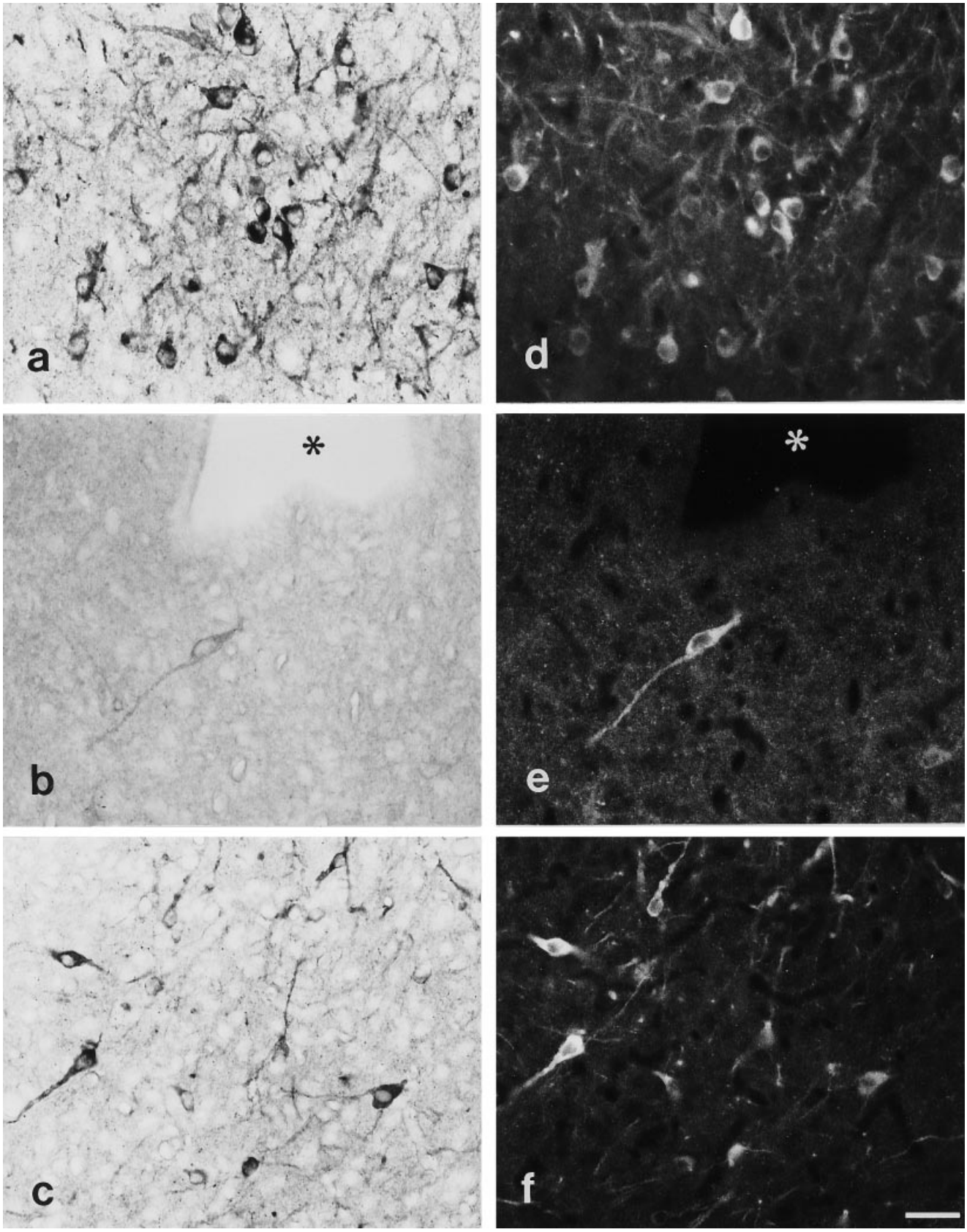

Fig. 6. Localization of nitric oxide synthase with nicotinamide-adenosine-dinucleotide phosphate diaphorase histochemistry (**a–c**) and immunocytochemistry (**d–f**). Photomicrographs of identical sections at higher magnification show a perfect match of reactive cell bodies in the ventrolateral nucleus (a,d) and in the arcuate nucleus at the anterior level (b,e) and posterior level (c,f). Asterisk, third ventricle. Scale bar = 35 µm for a,d, 23 µm for b,e, 40 µm for c,f.

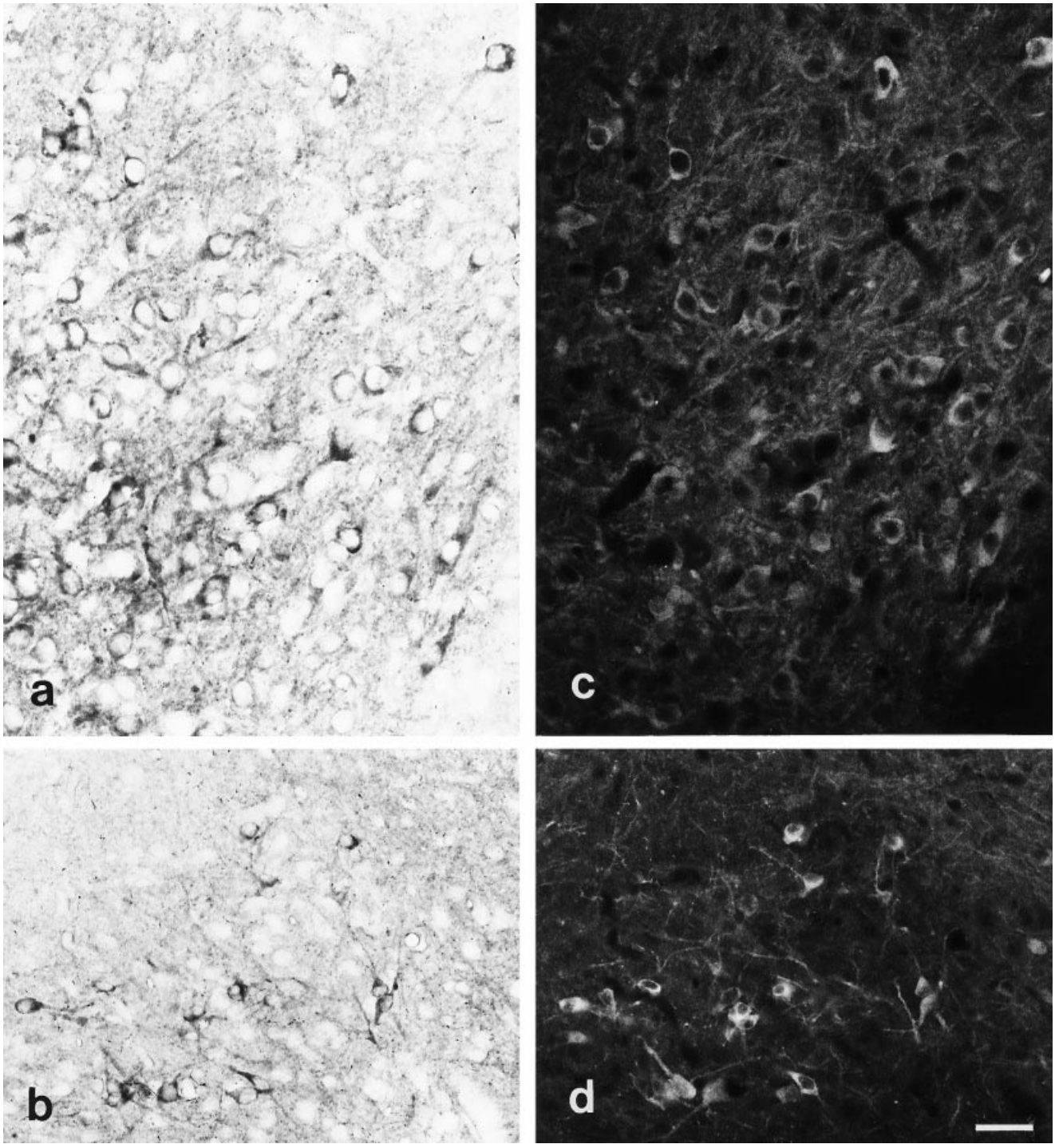

Fig. 7. Localization of nitric oxide synthase (NOS) with nicotinamide-adenosine-dinucleotide phosphate diaphorase (NADPHd) histochemistry (**a,b**) and immunocytochemistry (**c,d**). Photomicrographs of the same sections of the ventral premamillary nucleus (a,c) and the tuberal nucleus (b,d) show that almost every NADPHd-positive cell body is immunoreactive for NOS. Scale bar = 32 μm for a,c, 42 μm for b,d.

of NOS-IR cells in the rostral and 6% in the medial and caudal preoptic areas possessed PR, whereas only 0.44–0.90% of all PR-IR cells contained NOS (Table 1). The complete lack of double labeling in the anterior and medial regions of the arcuate nucleus was clearly due to the scarcity of NOS-IR cells (Fig. 10d). In the posterior part of the arcuate nucleus, NOS-positive cells lay intermingled with those staining for PR, but a very sporadic coexistence was seen in single neurons. NOS-IR neurons in the premamillary nucleus lacked PR immunoreactivity.

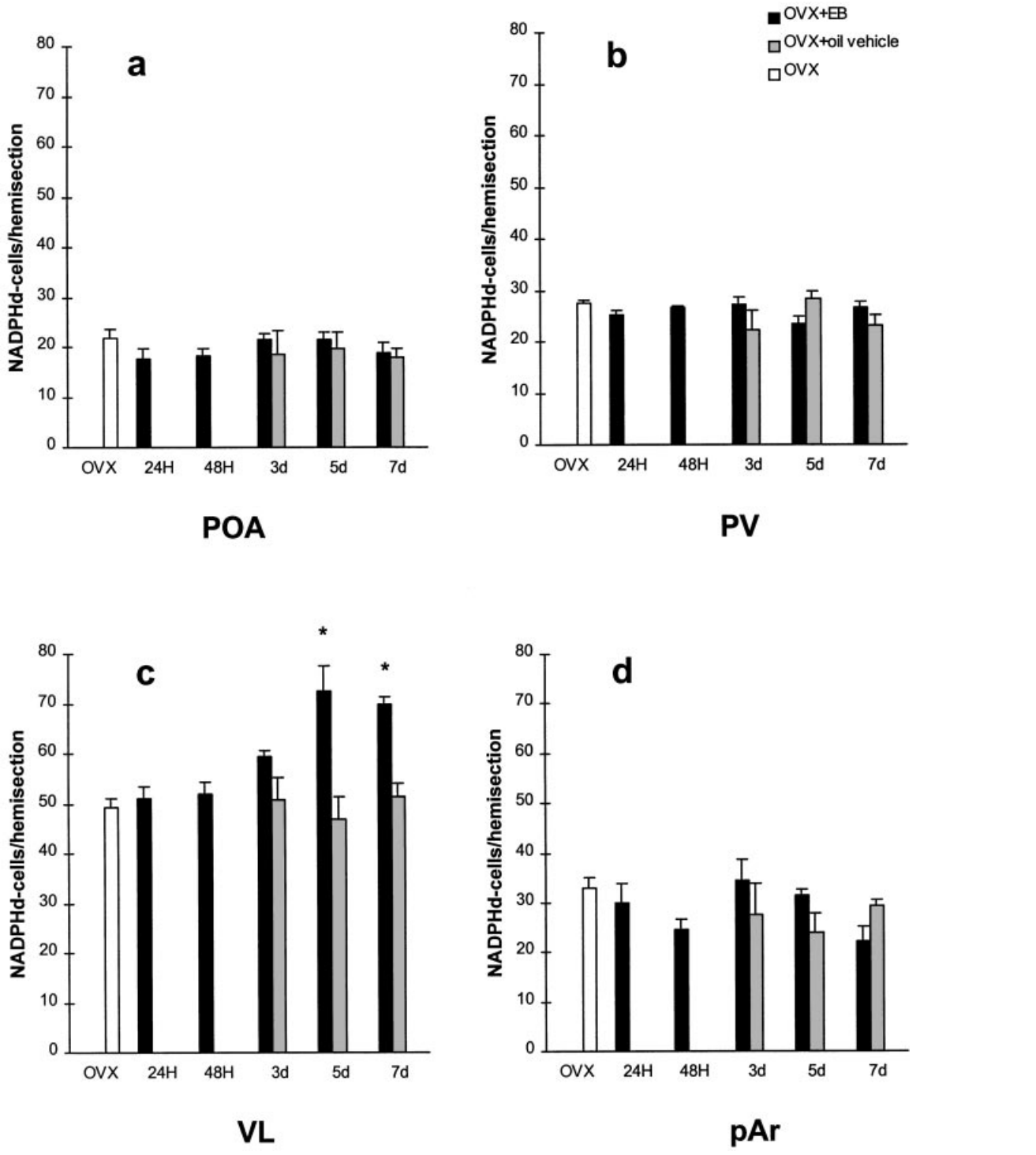

Fig. 8. **a–d:** Temporal effects of estradiol benzoate (EB) on the number of nicotinamide-adenosine-dinucleotide phosphate diaphorase–positive cells in the preoptic area (POA; a), in the paraventricular nucleus (PV; b), in the ventrolateral nucleus (VL; c), and in the posterior region of the arcuate nucleus (pAr; d). Bars represent the mean ± S.E.M. of cells per hemisection of brain regions from four guinea pigs (n = 4) by group: ovariectomized (OVX), OVX treated with 15 μg EB for 24 or 48 hours or 3, 5, or 7 days or with a sesame oil vehicle for 3, 5, or 7 days prior to death. Data were analyzed with an one-way analysis of variance (POA: $F[8,22] = 0.51$, $P = 0.83$; PV: $F[8,24] = 1.91$, $P = 0.11$; VL: $F[8,24] = 10.2$, $P < 0.0001$; pAr: $F[8,23] = 1.78$, $P = 0.14$) followed by the Bonferroni t-test. *Significantly different from OVX guinea pigs and OVX guinea pigs treated with the vehicle ($P < 0.05$).

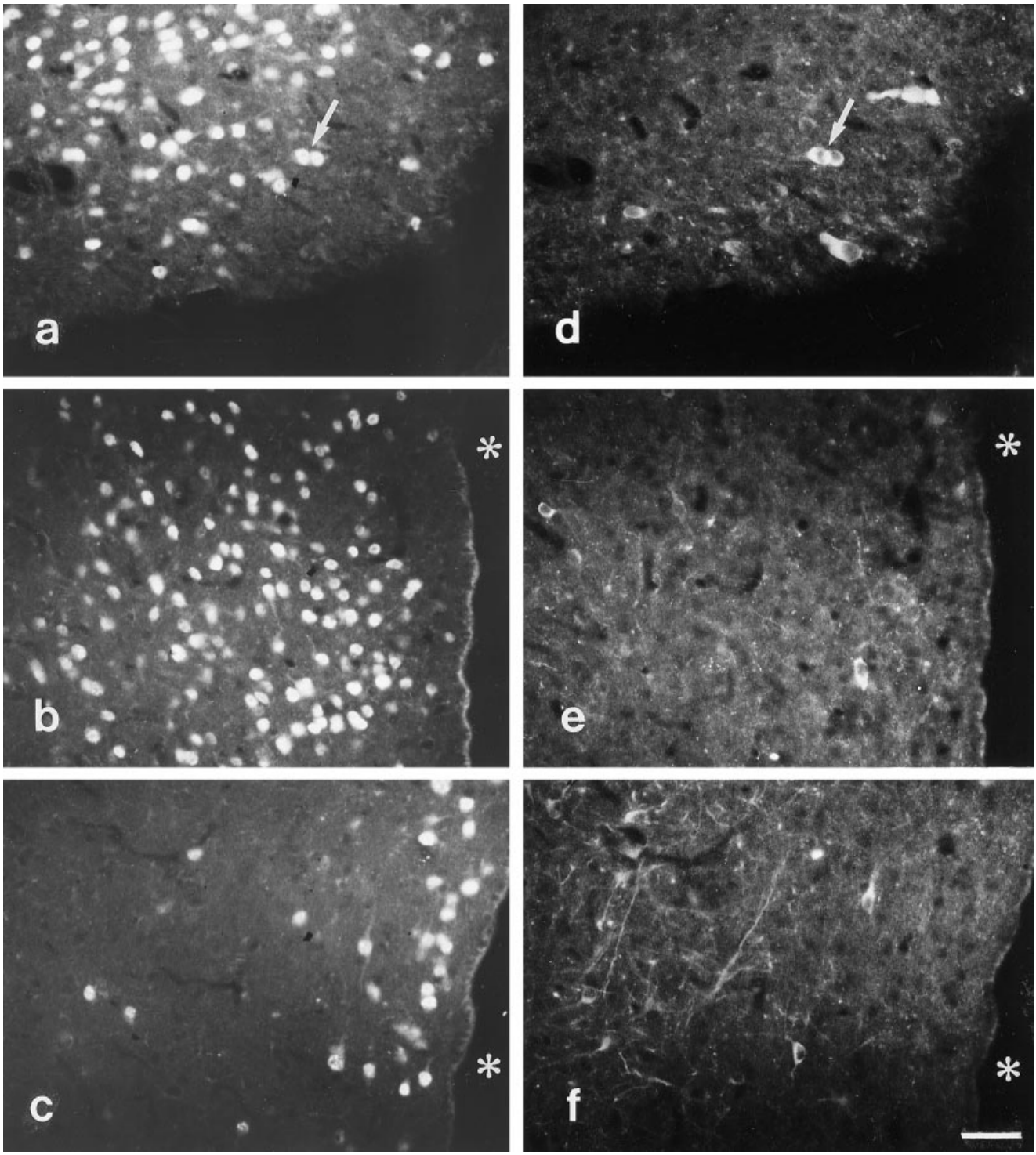

Fig. 9. Fluorescent photomicrographs of cross sections of the preoptic area show the distribution of progesterone receptor-immunoreactive (PR-IR) neurons (**a–c**) and the distribution of nitric oxide synthase (NOS)-IR neurons (**d–f**). The codistribution of both stainings is illustrated for the medial preoptic nucleus at the anterior level (a,d) and a more posterior level (b,e) and for the periventricular preoptic nucleus (c,f). The arrows in a and d indicate two adjacent cells containing both PR and NOS immunoreactivities. Asterisk, third ventricle. Scale bar = 42 μm for a,d, 71 μm for b,c,e,f.

Double-IR cells were found predominantly within the ventrolateral nucleus (Fig. 10e,f). This colocalization was consistent throughout the rostrocaudal extent of the nucleus. However, double-IR cells were slightly more abundant at the caudal level (Table 1). We estimated that approximately 55%, 53%, and 57% of NOS-IR neurons in

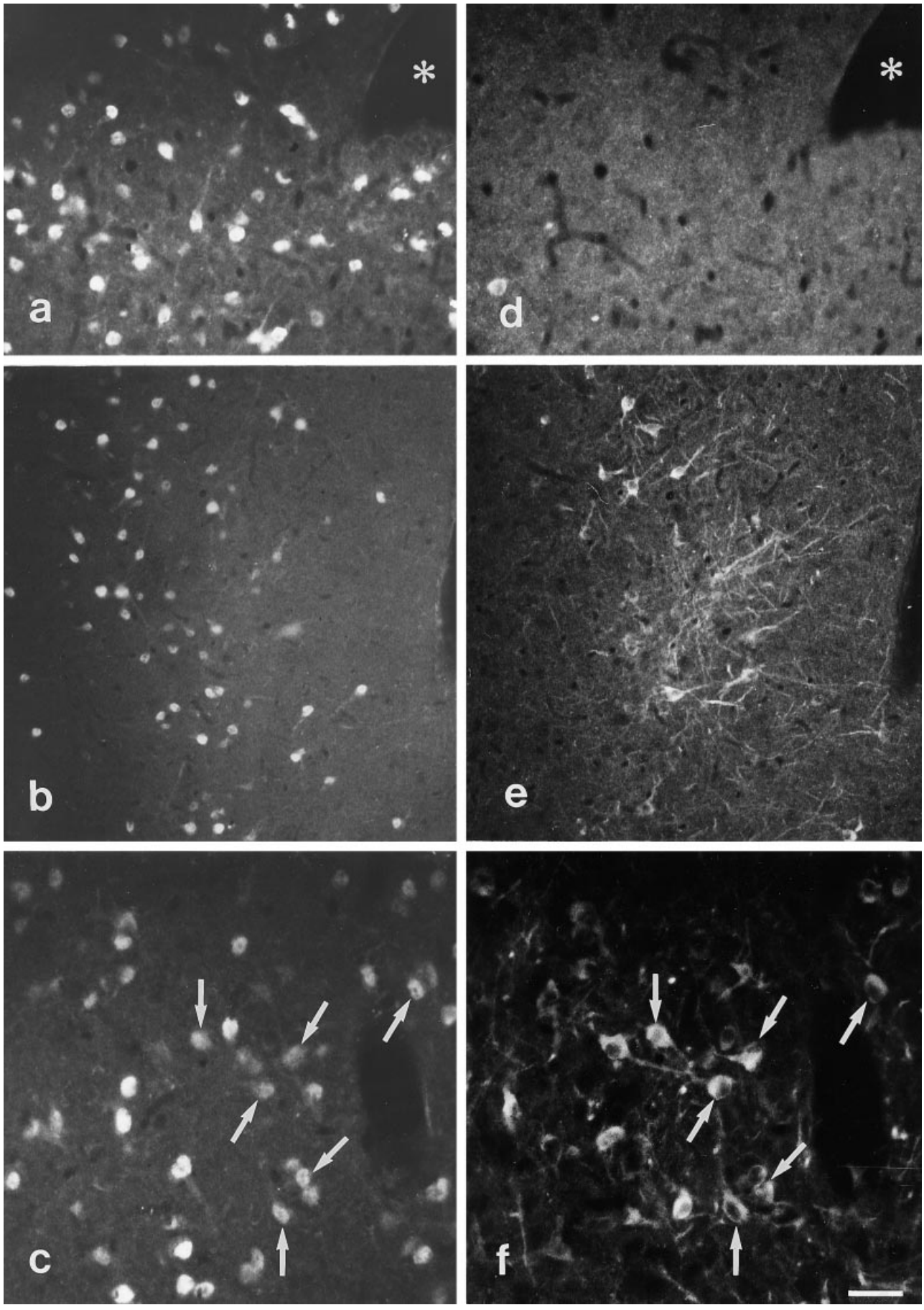

Figure 10

the rostral, medial, and caudal ventrolateral nucleus, respectively, possessed PR immunoreactivity and that NOS-IR cells accounted for 18–23% of all PR-IR cells in these regions (Table 1). Figure 11 illustrates the results of double staining for NOS and PR in different nuclei at high power magnification.

DISCUSSION

The present study has shown that NOS, the enzyme responsible for making the messenger NO, is expressed in a subpopulation of neurons throughout the guinea pig preoptic area and hypothalamus. Combining NADPHd histochemistry and NOS immunostaining in the same section showed that all NADPHd-reactive neurons are also NOS-IR. NADPHd activity is likely to result from neuronal NOS, which has been suggested to be the major NOS isoform in the hypothalamus (Bhat et al., 1996). Moreover, NADPHd-containing neurons were selectively labeled with a specific antibody that recognized neuronal NOS. It has been reported that fixation conditions affect the NADPHd activity and could lead to a lack of correlation between NADPHd labeling and NOS staining (Gonzalez-Hernandez et al., 1996). Fixation of brains with 4% paraformaldehyde alone, used in the present study, did not produce substantial differences in the diencephalic regions. As a whole, our results are consistent with those of previous studies that report a strong correlation between NADPHd histochemistry and NOS immunocytochemistry (Bredt et al., 1991; Dawson et al., 1991; Hope et al., 1991; Hashikawa et al., 1994).

To our knowledge, the present study is the first to detail the distribution of NADPHd-positive and NOS-IR cells in the preoptic area and hypothalamus of the guinea pig. Most of the results are in good agreement with the work of other laboratories about the distribution of NADPHd and NOS in the diencephalon of the rat (Vincent and Kimura, 1992; Rodrigo et al., 1994; Vanhatalo and Soinila, 1995), cat (Mizukawa et al., 1989), and monkey (Satoh et al., 1995). However, there are instances of differences in the distribution between species. These differences, in spite of the overwhelming similarities between the immunocytochemical and histochemical results, are related mainly to the magnocellular supraoptic and paraventricular nuclei and to the dorsomedial hypothalamic and arcuate nuclei. We found many NOS-positive neurons in the paraventricular nucleus but only a weak enzymatic activity in the supraoptic nucleus, although it could be detected in magnocellular neurons in the same sections, ruling out a technical problem. These nuclei are the most distinct NOS-IR and NADPHd-positive areas in the rat hypothalamus (Vincent and Kimura, 1992; Rodrigo et al., 1994; Vanhatalo and Soinila, 1995). In contrast, Satoh et al. (1995) reported that the supraoptic and paraventricular nuclei of the monkey did not contain NOS-IR cell bodies. In humans, Sangruchi and Kowall (1991) described that the paraventricular nucleus exhibited only scattered NADPHd-positive neurons and that the supraoptic nucleus was unstained. In the cat, NADPHd-positive neurons have been observed in the paraventricular nucleus, although their presence in the supraoptic nucleus has not been noted (Mizukawa et al., 1989). Our results demonstrated that immunoreactivity for NOS was present in the dorsal hypothalamic area. This distribution is comparable to that found in the rat (Vincent and Kimura, 1992) and in the cat (Mizukawa et al., 1989) following NADPHd histochemistry but differs from the absence of immunostaining noted in rat by Rodrigo et al. (1994). It is noteworthy that the many small NOS-IR cells detected by Satoh et al. (1995) in the arcuate nucleus of the macaque were not found in the guinea pig. The ventrolateral nucleus of the guinea pig contained many cells staining intensely for NADPHd or NOS. This finding appears to be in accordance with the situation within the area referred to as the ventrolateral part of the ventromedial hypothalamic nucleus in the rat (Okamura et al., 1994a). The preoptic area contained NOS-positive cells in all species examined to date. In spite of the close similarity in the general arrangement of NADPHd-positive neurons in the preoptic area of guinea pig and rat, the number of cells seemed greater in the rat (Okamura et al., 1994b) than in the guinea pig.

Our data demonstrated that NO may be synthesized in neurons throughout the brain of the guinea pig but that the distribution of NOS-positive neurons was not associated exclusively with a particular functional system. This finding raises the possibility of involvement of NO in different aspects of the central information processing, and it is generally accepted that many of the effects of NO are mediated by its effects on soluble guanylyl cyclase, which forms cyclic guanosine monophosphate in target cells (Garthwaite et al., 1988; Bredt and Snyder, 1989; Knowles et al., 1989; Snyder, 1992). NOS was expressed in many neurosecretory cells and nuclei, such as the preoptic and periventricular nuclei, the bed of nucleus of the stria terminalis, the ventrolateral nucleus, and the paraventricular and supraoptic nuclei, which are responsible, among other functions, for the regulation of reproductive processes.

Differential regulation of NOS has been shown to occur in the brain. Regulation of neuronal NOS mRNA has been reported in response to a variety of stimuli such as salt loading (Kadowaki et al., 1994), food or water deprivation (Ueta et al., 1995; O'Shea and Gundlach, 1996), and immobilization stress (Kishimoto et al., 1996) acting on hormone secretion. Sex hormones have been recently demonstrated to regulate constitutive NOS in both central and peripheral nervous systems (Weiner et al., 1994; Schirar et al., 1997). In the present study, the observed increase in the number of NADPHd-positive cells in the ventrolateral nucleus strongly suggests that NOS synthesis is stimulated in response to estrogen; thus, the generation of NO is likely to be enhanced in this region. A period of estrogenic impregnation of as long as 5 days was required for a significant elevation of NOS activity, suggesting a delayed action of estrogen. This result is in line with the findings of Okamura et al. (1994a) who showed a stimulatory effect of estrogen on NADPHd activity and with those of Ceccatelli et al. (1996) who showed an increase in neuronal NOS mRNA in the ventrolateral aspect of the ventromedial nucleus of the rat. In the other regions analyzed, the number of NADPHd-positive cells between OVX and EB-primed OVX animals was not significantly increased whatever the duration of treatment. However, the possibility that NO production may have been altered by estrogen treatment even through the

Fig. 10. Double-labeled sections for progesterone receptor-immunoreactivity (**a–c**) and nitric oxide synthase immunocytochemistry (**d–f**) through the anterior arcuate nucleus (a,d) and through the ventrolateral nucleus (b,c,e,f). Arrows indicate examples of double-immunoreactive neurons. Asterisk, third ventricle. Scale bar = 42 μm for a,d, 70 μm for b,e, 35 μm for c,f.

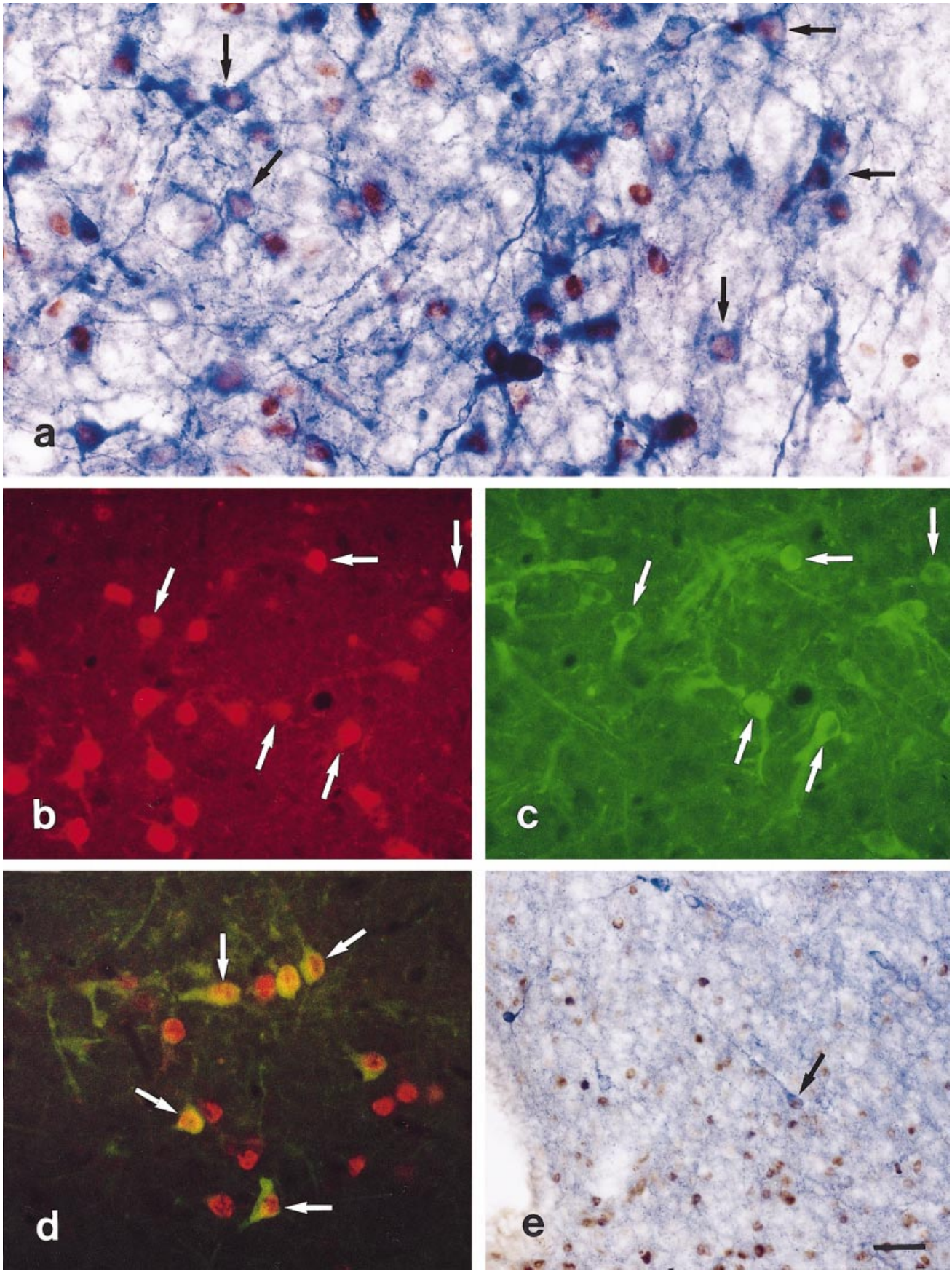

Figure 11

number of NADPHd-positive neurons was not changed cannot be completely ruled out. Our failure to find a drastic rise of NADPHd-positive cells in the preoptic area is not in accordance with the report of Okamura et al. (1994b), which showed an estrogenic induction of NADPHd activity in the medial preoptic nucleus of female rats in response to the EB treatment for 2 successive days. This discrepancy may reflect species differences in the distribution and regulation of NOS in the brain. The action of sex hormones seems to be regionally specific. It is interesting to note that NOS expression in the magnocellular neurons of the paraventricular and supraoptic nuclei was not affected by gonadal steroids. In these regions, NOS-positive neurons are regulated in an activity-dependent manner (Pow, 1992; O'Shea and Gundlach, 1996). In the rat, both water deprivation and salt loading increase NOS mRNA and NADPHd staining in these nuclei (Kadowaki et al., 1994; Ueta et al., 1995), whereas food deprivation is associated with a reduction of NOS gene expression (Ueta et al., 1995). Late pregnancy (Woodside and Amir, 1996) and lactation (Ceccatelli and Eriksson, 1993; Luckman et al., 1997) are also associated with an increase in NOS in both the paraventricular and supraoptic nuclei.

The present study provides, for the first time, direct evidence that NADPHd/NOS and PR are colocalized in a specific subpopulation of neurons in the guinea pig preoptic area and ventrolateral hypothalamic nucleus. Although the distribution of PR-IR neurons overlapped with NOS immunoreactivity, PR immunoreactivity was far more extensive than the distribution of NOS-IR cells, particularly in the preoptic area. There was also a region, the arcuate nucleus, in which NOS-IR neurons were almost undetectable and where, in contrast, PR-IR neurons were particularly abundant. Our quantification showed that approximately 6–16% of NOS-IR cells in the preoptic area and 55–57% in the ventrolateral nucleus contained PR. Cells containing both PR and NOS were estimated to account for 1% and 23%, respectively, of the PR population in these regions. It is likely that these double-IR cells also contain estrogen receptors because virtually all estradiol-induced PR-IR neurons in the diencephalon also express estrogen receptors (Warembourg et al., 1989). Our results are in concordance with those of Okamura et al. (1994b) and Rachman et al. (1996) who found a colocalization of NADPHd/NOS and estrogen receptors in neurons of the ventrolateral subdivision of the ventromedial nucleus of rat. However, the restricted coexistence of PR and NOS that we found in the preoptic area differs from that of Okamura et al. (1994a) who apparently observed a high number of NADPHd/estrogen receptor cells.

Fig. 11. Photomicrographs through the ventrolateral nucleus (**a–d**) and at the posterior level of the arcuate nucleus (**e**) after nicotinamide-adenosine-dinucleotide phosphate diaphorase (NADPHd) histochemistry combined with progesterone receptor (PR) immunocytochemistry (a,e) or after double-immunofluorescence immunocytochemistry with a PR antiserum and nitric oxide synthase (NOS) antiserum (b–d). Arrows indicate examples of double-stained neurons. In a and e, dual-stained neurons show both the purplish blue color typical of NADPHd staining in the perikarya and processes and the brown color of the immunoperoxidase reaction in nuclei. In b–d, double-immunoreactive cells exhibit PR immunoreactivity in their nucleus (red fluorescence from Texas red) and NOS immunoreactivity in their cytoplasm (green fluorescence from fluorescein) after switching from one filter cube to the other during the observation (b,c) and with a BGR filter (d). Scale bar = 20 μm for a, 35 μm for b–d, 75 μm for e.

At present, it is not fully understood what precise function NO may have in the preoptic area and ventrolateral nucleus. Recently, there has been considerable evidence in the literature that NO plays an important role in the regulation of GnRH secretion based on in vitro and in vivo studies using NO donors or NOS inhibitors (Bonavera et al., 1993, 1994; Moretto et al., 1993; Rettori et al. 1993; Lopez et al., 1997). The involvement of NO has been reported not only in the preovulatory luteinizing hormone (LH) surge but also in the progesterone-induced facilitation of the LH release in estradiol-primed OVX rats. GnRH release mediated by glutamate and norepinephrine may also involve NO (Pu et al., 1996). However, GnRH neurons in the preoptic area do not appear to stain for NOS, but they are frequently surrounded by NOS-producing perikarya (Bhat et al., 1995; Herbison et al., 1996). The absence of gonadal steroid receptors in the GnRH-containing neurons has started investigations of other neuromodulators or neurotransmitters that may be regulated by steroids, which in turn could act on the GnRH-containing neurons (Shivers et al., 1984; Herbison and Theodosis, 1992; Leranth et al., 1992; Watson et al., 1992). Multiple neurotransmitters and neuropeptides including γ-aminobutyric acid (Flügge et al., 1986), catecholamines (Warembourg et al., 1996), opioids (Simerly et al., 1996), neurotensin (Axelson et al., 1992; Herbison and Theodosis., 1992), and galanin (Bloch et al., 1992; Warembourg and Jolivet, 1993) have been identified in cells containing estrogen receptors and/or PR in the preoptic area. These neurochemical systems may be potential candidates for the transmission of gonadal steroid signals to GnRH cells. Our result of a colocalization of NOS in PR-IR neurons suggest that NO may mediate the effects of progesterone on synthesis, storage, and release of these chemicals by acting as a regulatory messenger molecule to modulate the synchronized GnRH discharge.

The colocalization of NOS and PR in the ventrolateral nucleus, a site at which local implantation of estradiol induces the appearance of PR and primes OVX guinea pigs to respond behaviorally to systemic progesterone administration (Delville and Blaustein, 1991), supports the notion that NOS is involved in the regulation of lordosis. Physiological studies have shown that NO is an essential mediator of lordosis behavior in female rats (Mani et al., 1994). Receptive behavior can be induced in estrogen-primed OVX rats with progesterone. When an inhibitor of NOS, N^G-monomethyl-L-arginine, was microinjected into the third ventricle of awake, estrogen-primed OVX rats prior to the injection of progesterone, lordosis was prevented (Mani et al., 1994). Microinjections of N^G-monomethyl-D-arginine, which does not inhibit NO production, did not inhibit lordosis under the same experimental conditions. Microinjections of sodium nitroprusside, a substance that spontaneously releases NO, mimicked the facilitative effect of progesterone on lordosis in estrogen-primed OVX rats. Microinjections of a GnRH antiserum can block lordosis facilitated by progesterone or sodium nitroprusside (Mani et al., 1994). Thus, progesterone seems to cause the release of NO that stimulates GnRH secretion from the hypothalamus, which subsequently may mediate receptive behavior. It is highly likely that the NOS-producing and PR-containing neurons found in the ventrolateral nucleus are associated with the NO-mediated regulation of lordosis. Receptive behavior may also be regulated by several neurotransmitter or neuromodulator systems. Because substance P (Nielsen and Blaustein,

1990; Dufourny et al., 1998), neurotensin (Warembourg and Jolivet, 1994), and somatostatin (Dufourny and Warembourg, 1996) have been shown to colocalize to different degrees with the PR in the guinea pig ventrolateral nucleus, it is conceivable that at least some of the NOS-containing neurons also contain these substances. The possible presence of NOS within these systems suggests that NO has the potential to modulate the activity of one or both of these neuronal networks and adds to our understanding of the neurochemistry of lordosis.

In conclusion, the present study demonstrates that NADPHd staining parallels NOS immunoreactivity of the preoptic area and hypothalamus of the guinea pig. EB treatment results in a significant increase in the number of NADPHd-positive neurons in the ventrolateral nucleus. Our results provide neuroanatomical evidence that a subpopulation of NOS-producing neurons is capable of binding progesterone in the preoptic area and ventrolateral nucleus. The close relationship of NOS with steroid target neurons in these regions suggests that NOS modulates ovarian steroid responsiveness through direct effects on neurons containing steroid receptors or by diffusion of NO to neighboring steroid responsive neurons. Thus, NO may operate as an important chemical signal for intercellular communication and may play a fundamental role in neuroendocrine functions and behavior.

ACKNOWLEDGMENT

We thank Prof. J.M. Polak (Department of Histochemistry, Hammersmith Hospital, London, U.K.) for generously providing the NOS antiserum.

LITERATURE CITED

Axelson JF, Shannon W, Van Leeuwen FW. 1992. Immunocytochemical localization of estrogen receptors within neurotensin cells in the rostral preoptic area of the rat hypothalamus. Neurosci Lett 136:5–9.

Bhat G, Mahesh VB, Lamar CA, Ping L, Aguan K, Brann DW. 1995. Histochemical localization of nitric oxide neurons in the hypothalamus: association with gonadotropin-releasing hormone neurons and co-localization with N-methyl-D-aspartate receptors. Neuroendocrinology 62:187–197.

Bhat G, Mahesh VB, Aguan K, Brann DW. 1996. Evidence that brain nitric oxide synthase is the major nitric oxide synthase isoform in the hypothalamus of the adult female rat and that nitric oxide potently regulates hypothalamic cGMP levels. Neuroendocrinology 64:93–102.

Blaustein JD, King JC, Toft DO, Turcotte J. 1988. Immunocytochemical localization of estrogen-induced progestin receptors in the guinea-pig brain. Brain Res 474:1–15.

Bleier R. 1983. The hypothalamus of the guinea pig. A cytoarchitectonic atlas. Madison: University of Wisconsin Press.

Bloch GJ, Kurth SM, Akesson TR, Micevych PE. 1992. Estrogen-concentrating cells within cell groups of the medial preoptic area: sex differences and co-localization with galanin-immunoreactive cells. Brain Res 595:301–308.

Bonavera JJ, Sahu A, Kalra PS, Kalra SP. 1993. Evidence that nitric oxide may mediate the ovarian steroid induced luteinizing hormone surge: involvement of excitatory amino acids. Endocrinology 133:2481–2487.

Bonavera JJ, Sahu A, Kalra PS, Kalra SP. 1994. Evidence in support of nitric oxide (NO) involvement in the cyclic release of prolactin and LH surge. Brain Res 660:175–179.

Bredt DS, Snyder SH. 1989. Nitric oxide mediates glutamate-linked enhancement of cGMP levels in the cerebellum. Proc Natl Acad Sci USA 86:9030–9033.

Bredt DS, Snyder SH. 1990. Isolation of nitric oxide synthase, a calmodulin-requiring enzyme. Proc Natl Acad Sci USA 87:682–685.

Bredt DS, Snyder SH. 1992. Nitric oxide, a novel neuronal messenger. Neuron 8:3–11.

Bredt DS, Glatt CE, Hwang PM, Fotuhi M, Dawson TM, Snyder SH. 1991. Nitric oxide synthase protein and mRNA are discretely localized in neuronal populations of the mammalian CNS together with NADPH diaphorase. Neuron 7:615–624.

Ceccatelli S, Eriksson M. 1993. The effect of lactation on nitric oxide synthase gene expression. Brain Res 625:177–179.

Ceccatelli S, Grandison L, Scott REM, Pfaff DW, Kow LM. 1996. Estradiol regulation of nitric oxide synthase mRNAs in rat hypothalamus. Neuroendocrinology 64:357–363.

Dawson TM, Bredt DS, Fotuhi M, Hwang PH, Snyder SH. 1991. Nitric oxide synthase and neuronal NADPH diaphorase are identical in brain and peripheral tissues. Proc Natl Acad Sci USA 88:7797–7801.

Delville Y, Blaustein JD. 1991. A site for estradiol priming of progesterone-facilitated sexual receptivity in the ventrolateral hypothalamus of female guinea pigs. Brain Res 559:191–199.

Don Carlos LL, Greene GL, Morrell JI. 1989. Estrogen plus progesterone increases progestin receptor immunoreactivity in the brain of ovariectomized guinea-pigs. Neuroendocrinology 50:613–623.

Dufourny L, Warembourg M. 1996. Colocalization of progesterone receptor and somatostatin immunoreactivities in the hypothalamus of the male and female guinea pig. Neuroendocrinology 64:215–224.

Dufourny L, Warembourg M, Jolivet A. 1998. Multiple peptides infrequently coexist in progesterone receptor-containing neurons in the ventrolateral hypothalamic nucleus of the guinea pig: an immunocytochemical triple-label analysis of somatostatin, neurotensin and substance P. J Neuroendocrinol 10:165–173.

Egberongbe YI, Gentleman SM, Falkai P, Bogerts B, Polak JM, Roberts GW. 1994. The distribution of nitric oxide synthase immunoreactivity in the human brain. Neuroscience 59:561–578.

Flügge G, Oertel WH, Wuttke W. 1986. Evidence for estrogen-receptive GABAergic neurons in the preoptic/anterior hypothalamic area of the rat brain. Neuroendocrinology 43:1–5.

Forstermann U, Schmidt HH, Pollock JS, Sheng H, Mitchell JA, Warner TD, Nakane M, Murad F. 1991. Isoforms of nitric oxide synthase. Characterization and purification from different cell types. Biochem Pharmacol 442:1849–1857.

Garhwaite J, Charles SL, Chess-Williams R. 1988. Endothelium-derived relaxing factor release on activation of NMDA receptors suggests role as intercellular messenger in the brain. Nature 336:385–388.

Gonzalez-Hernandez T, Perez De La Cruz MA, Mantolan-Sarmiento B. 1996. Histochemical and immunohistochemical detection of neurons that produce nitric oxide: effect of different fixative parameters and immunoreactivity against non-neuronal NOS antisera. J Histochem Cytochem 44:1399–1413.

Hashikawa T, Leggio MG, Hattori R, Yui Y. 1994. Nitric oxide synthase immunoreactivity colocalized with NADPH-diaphorase histochemistry in monkey cerebral cortex. Brain Res 641:341–349.

Herbison AE, Theodosis DT. 1992. Localization of estrogen receptors in preoptic neurons containing neurotensin but not tyrosine hydroxylase, cholecystokinin or luteinizing hormone-releasing hormone in the male and female rat. Neuroscience 50:283–298.

Herbison AE, Simonian SX, Norris PJ, Emson PC. 1996. Relationship of neuronal nitric oxide synthase immunoreactivity to GnRH neurons in the ovariectomized and intact female rat. J Neuroendocrinol 8:73–82.

Hope BT, Michael GJ, Knigge LM, Vincent SR. 1991. Neuronal NADPH diaphorase is a nitric oxide synthase. Proc Natl Acad Sci USA 88:2811–2814.

Kadowaki K, Kishimoto J, Leng G, Emson PC. 1994. Up-regulation of nitric oxide synthase (NOS) gene expression together with NOS activity in the rat hypothalamo-hypophysial system after chronic salt loading: evidence of a neuromodulatory role of nitric oxide in arginine vasopressin and oxytocin secretion. Endocrinology 134:1011–1017.

Kharazia VN, Schmidt HHHW, Weinberg RJ. 1994. Type I nitric oxide synthase fully accounts for NADPH-diaphorase in rat striatum, but not cortex. Neuroscience 62:983–987.

Kishimoto J, Tsuchiya T, Emson PC, Nakayama Y. 1996. Immobilization-induced stress activates neuronal nitric oxide synthase (nNOS) mRNA and protein in hypothalamic–pituitary–adrenal axis in rats. Brain Res 720:159–171.

Knowles RG, Palacios M, Palmer RMJ, Moncada S. 1989. Formation of nitric oxide from L-arginine in the central nervous system: a transduction mechanism for stimulation of the soluble guanylate cyclase. Proc Natl Acad Sci USA 86:5159–5162.

Kuonen DR, Kemp MC, Roberts PJ. 1988. Demonstration and biochemical characterization of rat brain NADPH-dependent diaphorase. J Neurochem 50:1017–1025.

Leranth C, MacLusky NJ, Brown TJ, Chen EC, Redmond DE Jr, Naftolin F. 1992. Transmitter content and afferent connections of estrogen-

sensitive progestin receptor-containing neurons in the primate hypothalamus. Neuroendocrinology 55:667–682.

Logeat F, Vu Hai MT, Fournier A, Legrain P, Butin P, Milgrom E. 1983. Monoclonal antibodies to rabbit progesterone receptor: cross-reaction with other mammalian progesterone receptors. Proc Natl Acad Sci USA 80:6456–6459.

Logeat F, Pamphile R, Loosfelt H, Jolivet A, Fournier A, Milgrom E. 1985. One-step immunoaffinity purification of active progesterone receptor. Further evidence in favor of the existence of a single steroid-binding subunit. Biochemistry 24:1029–1035.

Loosfelt H, Logeat F, Vu Hai MT, Milgrom E. 1984. The rabbit progesterone receptor. Evidence for a single steroid-binding subunit and characterization of receptor mRNA. J Biol Chem 259:14196–14202.

Lopez FJ, Moretto M, Merchenthaler I, Negro-Vilar A. 1997. Nitric oxide is involved in the genesis of pulsatile LHRH secretion from immortalized LHRH neurons. J Neuroendocrinol 9:647–654.

Lorenzo F, Jolivet A, Loosfelt H, Vu Hai MT, Brailly S, Perrot-Applanat M, Milgrom E. 1988. A rapid method of epitope mapping. Application to the study of immunogenic domains and to the characterization of various forms of rabbit progesterone receptor. Eur J Biochem 176:53–60.

Luckman SM, Huckett L, Bicknell RJ, Voisin DL, Herbison AE. 1997. Up-regulation of nitric oxide synthase messenger RNA in an integrated forebrain circuit involved in oxytocin secretion. Neuroscience 77:37–48.

Mani SK, Allen JMC, Rettori V, McCann SM, O'Malley BW, Clark JH. 1994. Nitric oxide mediates sexual behavior in female rats. Proc Natl Acad Sci USA 91:6468–6472.

Martinez A, Riveros-Moreno V, Polak JM, Moncada S, Sesma P. 1994. Nitric oxide (NO) synthase-immunoreactivity in the starfish *Marthasterias gracilis*. Cell Tissue Res 275:599–603.

Mayer B, John M, Böhme E. 1990. Purification of a Ca^{2+}/calmodulin-dependent nitric oxide synthase from porcine cerebellum. FEBS Lett 277:215–219.

Mayer B, Koesling D, Böhme E. 1993. Characterization of nitric oxide synthase, soluble guanylyl cyclase, and Ca^{2+}/calmodulin-stimulated cGMP phosphodiesterase as components of neuronal signal transduction. Adv Second Messeng Phosphoprot Res 28:111–119.

Mizukawa K, Vincent SR, McGeer PL, McGeer EG. 1989. Distribution of reduced-nicotinamide-adenine-dinucleotide phosphate diaphorase-positive cells and fibers in the cat central nervous system. J Comp Neurol 279:281–311.

Moretto M, Lopez FJ, Negro-Vilar A. 1993. Nitric oxide regulates luteinizing hormone-releasing hormone secretion. Endocrinology 133:2399–2402.

Nelson RJ, Demas GE, Huang PL, Fishman MC, Dawson VL, Dawson TM, Snyder SH. 1995. Behavioural abnormalities in male mice lacking neuronal nitric oxide synthase. Nature 378:383–386.

Nielsen KH, Blaustein JD. 1990. Many progestin receptor-containing neurons in the guinea pig ventrolateral hypothalamus contain substance P: immunocytochemical evidence. Brain Res 517:175–181.

O'Shea RD, Gundlach AL. 1996. Food or water deprivation modulate nitric oxide synthase (NOS) activity and gene expression in rat hypothalamic neurones: correlation with neurosecretory activity. J Neuroendocrinol 8:417–425.

Okamura H, Yokosuka M, Hayashi S. 1994a. Estrogenic induction of NADPH-diaphorase activity in the preoptic neurons containing estrogen receptor immunoreactivity in the female rat. J Neuroendocrinol 6:597–601.

Okamura H, Yokosuka M, McEwen BS, Hayashi S. 1994b. Colocalization of NADPH-diaphorase and estrogen receptor immunoreactivity in the rat ventromedial hypothalamic nucleus: stimulatory effect of estrogen on NADPH-diaphorase activity. Endocrinology 135:1705–1708.

Pow DV. 1992. NADPH-diaphorase (nitric oxide synthase) staining in the rat supraoptic nucleus is activity-dependent: possible functional implications. J Neuroendocrinol 4:377–380.

Pu S, Xu B, Kalra SP, Kalra PS. 1996. Evidence that gonadal steroids modulate nitric oxide efflux in the medial preoptic area: effects of N-methyl-D-aspartate and correlation with luteinizing hormone secretion. Endocrinology 137:1949–1955.

Rachman IM, Pfaff DW, Cohen RS. 1996. NADPH diaphorase activity and nitric oxide synthase immunoreactivity in lordosis-relevant neurons of the ventromedial hypothalamus. Brain Res 740:291–306.

Rettori V, Belova N, Dees W, Nyberg C, Gimeno M, McCann SM. 1993. Role of nitric oxide in the control of luteinizing hormone-releasing hormone release *in vivo* and *in vitro*. Proc Natl Acad Sci USA 90:10130–10134.

Riveros-Moreno V, Bedell C, Moncada S. 1993. Nitric oxide synthase. Structural studies using auto-peptides antibodies. Eur J Biochem 215:801–808.

Rodrigo J, Springall DR, Uttenthal O, Bentura ML, Abadia-Molina F, Riveros-Moreno V, Martinez-Murillo R, Polak JM, Moncada S. 1994. Localization of nitric oxide synthase in the adult rat brain. Phil Trans R Soc Lond B 345:175–221.

Sangruchi T, Kowall NW. 1991. NADPH diaphorase histochemistry of the human hypothalamus. Neuroscience 40:713–724.

Satoh K, Arai R, Ikemoto K, Narita M, Nagai T, Ohshima H, Kitahama K. 1995. Distribution of nitric oxide synthase in the central nervous system of *Macaca fuscata*: subcortical regions. Neuroscience 66:685–696.

Schirar A, Bonnefond C, Meusnier C, Devinoy E. 1997. Androgens modulate nitric oxide synthase messenger ribonucleic acid expression in neurons of the major pelvic ganglion in the rat. Endocrinology 138:3093–3102.

Schmidt HHHW, Gagne GD, Nakane M, Pollock JS, Miller MF, Murad F. 1992. Mapping of neural nitric oxide synthase in the rat suggests frequent co-localization with NADPH diaphorase but not with soluble guanylyl cyclase, and novel paraneural functions for nitrinergic signal transduction. J Histochem Cytochem 40:1439–1456.

Shivers BD, Harlan RE, Morrell JI, Pfaff DW. 1984. Absence of estradiol concentration in cell nuclei of LHRH-immunoreactive neurons. Nature 304:345–347.

Simerly RB, Young BJ, Carr AM. 1996. Co-expression of steroid hormone receptors in opioid peptide-containing neurons correlates with patterns of gene expression during the estrous cycle. Mol Brain Res 40:275–284.

Snyder SH. 1992. Nitric oxide: first in a new class of neurotransmitters? Science 257:494–496.

Springall DR, Riveros-Moreno V, Buttery L, Suburo A, Bishop AE, Merrett M, Moncada S, Polak JM. 1992. Immunological detection of nitric oxide synthase(s) in human tissues using heterologous antibodies suggesting different isoforms. Histochemistry 98:259–266.

Terenghi G, Riveros-Moreno V, Hudson LD, Ibrahim NBN, Polak JM. 1993. Immunocytochemistry of nitric oxide synthase demonstrates immunoreactive neurons in spinal cord and dorsal root ganglia of man and rat. J Neurol Sci 118:34–37.

Thomas E, Pearse AGE. 1961. The fine localization of dehydrogenases in the nervous system. Histochemie 2:266–282.

Ueta Y, Levy A, Chowdrey HS, Lightman SL. 1995. Inhibition of hypothalamic nitric oxide synthase gene expression in the rat paraventricular nucleus by food deprivation is independent of serotonin depletion. J Neuroendocrinol 7:861–865.

Valtschanoff JG, Weinberg RJ, Kharazia VN, Nakane M, Schmidt HHHW. 1993. Neurons in rat hippocampus that synthesize nitric oxide. J Comp Neurol 331:111–121.

Vanhatalo S, Soinila S. 1995. Nitric oxide synthase in the hypothalamo-pituitary pathways. J Chem Neuroanat 8:165–173.

Vincent SR, Kimura H. 1992. Histochemical mapping of nitric oxide synthase in the rat brain. Neuroscience 46:755–784.

Warembourg M, Deneux D, Krieger M, Jolivet A. 1996. Progesterone receptor immunoreactivity in aromatic L-amino decarboxylase-containing neurons of the guinea pig hypothalamus and preoptic area. J Comp Neurol 367:477–490.

Warembourg M, Jolivet A. 1993. Immunocytochemical localization of progesterone receptors in galanin neurons in the guinea pig hypothalamus. J Neuroendocrinol 5:487–491.

Warembourg M, Jolivet A. 1994. Progesterone receptor and neurotensin are colocalized in neurons of the guinea pig ventrolateral hypothalamus. Neuroendocrinology 60:486–492.

Warembourg M, Logeat F, Milgrom E. 1986. Immunocytochemical localization of progesterone receptor in the guinea pig central nervous system. Brain Res 384:121–131.

Warembourg M, Jolivet A, Milgrom E. 1989. Immunohistochemical evidence of the presence of estrogen and progesterone receptors in the same neurons of the guinea pig hypothalamus and preoptic area. Brain Res 480:1–15.

Watson RE Jr, Langub MC Jr, Landis JW. 1992. Further evidence that most luteinizing hormone-releasing hormone neurons are not directly estrogen-responsive: simultaneous localization of luteinizing hormone-releasing hormone and estrogen receptor immunoreactivity in the guinea pig brain. J Neuroendocrinol 4:311–317.

Weiner CP, Lizasoain I, Baylis SA, Knowles RG, Charles IG, Moncada S. 1994. Induction of calcium-dependent nitric oxide synthases by sex hormones. Proc Natl Acad Sci USA 91:5212–5216.

Woodside B, Amir S. 1996. Reproductive state changes NADPH-diaphorase staining in the paraventricular and supraoptic nuclei of female rats. Brain Res 739:339–342.